7-2002

Volatiles in Basaltic Glasses from the Easter-Salas y Gomez Seamount Chain and Easter Microplate: Implications for Geochemical Cycling of Volatile Elements

Kyla Simons
University of Miami

Jacqueline Dixon
University of Miami, jdixon@usf.edu

Jean-Guy Schilling
University of Rhode Island

Richard Kingsley
University of Rhode Island

Robert Poreda
University of Rochester

Geochemistry Geophysics Geosystems G3
AN ELECTRONIC JOURNAL OF THE EARTH SCIENCES
Published by AGU and the Geochemical Society

Article
Volume 3, Number 7
9 July 2002
10.1029/2001GC000173
ISSN: 1525-2027

Volatiles in basaltic glasses from the Easter-Salas y Gomez Seamount Chain and Easter Microplate: Implications for geochemical cycling of volatile elements

Kyla Simons
Division of Marine Geology and Geophysics, Rosenstiel School of Marine and Atmospheric Science, University of Miami, 4600 Rickenbacker Causeway, Miami, Florida 33149, USA

Currently at Lamont-Doherty Earth Observatory, P.O. Box 1000, 61 Route 9W, Palisades, New York 10964-1000, USA (ksimons@ldeo.columbia.edu)

Jacqueline Dixon
Division of Marine Geology and Geophysics, Rosenstiel School of Marine and Atmospheric Science, University of Miami, 4600 Rickenbacker Causeway, Miami, Florida 33149, USA (jdixon@rsmas.miami.edu)

Jean-Guy Schilling and Richard Kingsley
Graduate School of Oceanography, University of Rhode Island, Narragansett, Rhode Island 02882-1197, USA (jgs@gso.uri.edu; kingsley@gso.uri.edu)

Robert Poreda
Department of Earth and Environmental Sciences, University of Rochester, Rochester, New York 14627, USA (poreda@siena.earth.rochester.edu)

[1] We present H_2O, CO_2, and Cl concentrations in 66 basaltic glasses from the Easter Microplate (EMP) and Easter-Salas y Gomez Seamount Chain (ESC) system in the southeastern Pacific. The EMP-ESC system is characterized by binary mixing between a depleted mid-ocean ridge basalt (MORB) mantle source (DMM) and an incompatible element and radiogenic isotope enriched source, the Salas y Gomez mantle plume (SyG). Plume material is channeled toward the ridge crest centered at ~27°S on the east rift of the microplate. Water concentrations on the EMP are highest on the east rift at ~27°S and become progressively lower to the north and south, following the spatial pattern of other geochemical tracers. EMP basalts have not lost H_2O to degassing but have assimilated variable quantities of a Cl-rich hydrothermal component. In contrast, some seamount basalts have lost water by shallow degassing, but very few have gained Cl, indicating little assimilation of Cl-rich materials. Several ESC seamount glasses may have assimilated a hydrous component, for example, serpentinized harzburgite, during magma ascent through the lithosphere. On the basis of samples unaffected by shallow processes, the main plume component has H_2O/Ce of ~210 ± 20 and is neither preferentially enriched nor depleted in H_2O relative to other similarly incompatible elements. The depleted MORB source has H_2O/Ce of ~150 ± 10. Estimated mantle volatile concentrations are 750 ± 210 ppm H_2O and 40 ± 11 ppm Cl for the SyG source, 120 ± 27 ppm H_2O and 4.5 ± 1.4 ppm Cl for an average EPR source, and 54 ± 12 ppm H_2O and 1.7 ± 0.4 ppm Cl for the DMM source. The coupled behavior of H_2O and Cl with similarly incompatible elements, coupled with elevated $^3He/^4He$ ratios, suggests that the volatiles are dominantly juvenile, representative of a component common to mantle plumes, with minor contribution from recycled lithospheric components.

Components: 15,455 words, 15 figures, 1 table.

Keywords: Easter; mantle plume; volatiles; water; chlorine; basalt.

Index Terms: 1020 Geochemistry: Composition of the crust; 1025 Geochemistry: Composition of the mantle; 1030 Geochemistry: Geochemical cycles (0330); 1065 Geochemistry: Trace elements (3670).

Received 30 April 2001; **Revised** 3 February 2002; **Accepted** 22 February 2002; **Published** 9 July 2002.

Simons, K., J. Dixon, J.-G. Schilling, R. Kingsley, and R. Poreda, Volatiles in basaltic glasses from the Easter-Salas y Gomez Seamount Chain and Easter Microplate: Implications for geochemical cycling of volatile elements, *Geochem. Geophys. Geosyst.*, *3*(7), 10.1029/2001GC000173, 2002.

1. Introduction

[2] Water and carbon dioxide are the two most abundant volatiles in the Earth's mantle [e.g., *Wood et al.*, 1990; *Tajika*, 1998]. They play important roles in mantle melting processes [*Green and Ringwood*, 1967; *Kushiro et al.*, 1968; *Kushiro*, 1970; *Green*, 1972, 1973; *Green and Wallace*, 1988], viscosity and buoyancy of mantle materials [*Dingwell and Mysen*, 1985; *Lange*, 1994; *Richet et al.*, 1996; *Hirth and Kohlstedt*, 1996; *Ito et al.*, 1999], explosivity of volcanoes [*Vergniolle and Jaupart*, 1986, 1990; *Head and Wilson*, 1987; *Greenland et al.*, 1988; *Cashman and Mangan*, 1994; *Sparks et al.*, 1994], origin of the atmosphere and ocean during outgassing of the early Earth [*Jambon*, 1994; *Javoy*, 1998] and are essential to life on this planet.

[3] Radiogenic isotopic compositions, combined with major and trace element concentrations, have been used to identify distinct mantle source regions [e.g., *Zindler and Hart*, 1986; *Hart*, 1988; *Hofmann*, 1988; *Sun and McDonough*, 1989; *Weaver*, 1991], including mantle that is both enriched (EM1, EM2, HIMU) and depleted (DMM) relative to estimates of the bulk silicate mantle. In addition, mantle plumes may contain a common component, variously termed PHEM [*Farley et al.*, 1992], FOZO [*Hart et al.*, 1992; *Hauri et al.*, 1994], or C [*Hanan and Graham*, 1996] used here. The distinct chemical signatures of enriched mantle end-members may be related to addition of coherent packages of subducted lithosphere to lower mantle material that is less depleted and less degassed than DMM. Recycled components may contain pelagic sediment, continental detritus, hydrothermal deposits, delaminated subcontinental mantle or altered oceanic crust + lithosphere [*White and Hofmann*, 1982; *Zindler et al.*, 1982; *Weaver*, 1991; *Chauvel et al.*, 1992; *Lassiter and Hauri*, 1998; *Blichert-Toft et al.*, 1999; *Douglass et al.*, 1999; *Kamenetsky et al.*, 2001; *Andres*, 2001]. Although substantial work has been done to identify the radiogenic and noble gas isotopic compositions of various mantle components, much less has been done to constrain their volatile concentrations [e.g., *Schilling et al.*, 1980; *Poreda et al.*, 1986; *Jambon and Zimmermann*, 1990; *Jambon*, 1994; *Michael*, 1995; 1999; *Dixon et al.*, 1997; *Wallace*, 1998; *Dixon and Clague*, 2001]. One approach is to study submarine basalts, where much of the initial volatile content is retained within quenched glassy rinds as exsolved (vesicles) or dissolved species. However, shallow level processes, such as degassing and assimilation, must be considered before extrapolating magmatic volatile variations to mantle processes [e.g., *Dixon et al.*, 1997; *Dixon and Clague*, 2001].

[4] The Easter Microplate-Easter-Salas y Gomez Seamount Chain is ideal for studying the variation of volatiles within different mantle source regions, because (1) submarine eruption likely preserves preeruptive water concentrations, (2) major and trace elements, as well as radiogenic and stable isotopes, show clear evidence of binary mixing between a depleted MORB source and an enriched source, possibly containing recycled basaltic crust, and (3) the mixing proportions of depleted and enriched sources varies systematically along the ridge axis and along the seamount chain [*Schilling et al.*, 1985; *Kingsley and Schilling*, 1998; *Pan and Batiza*, 1998; *Cheng et al.*, 1999; *Kingsley et al.*, 2002]. In this paper, we present new volatile data

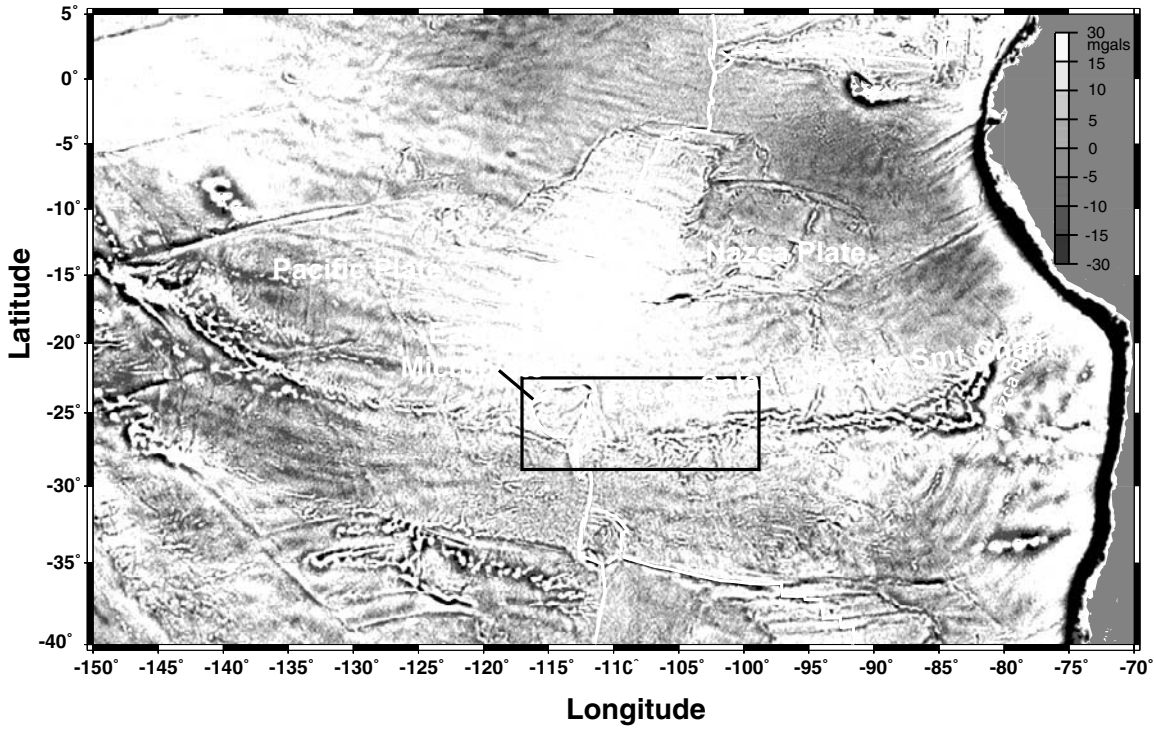

Figure 1. Free air gravity anomaly map for the South Pacific calculated from Geosat altimeter data [*Smith and Sandwell*, 1994]. Black rectangle indicates study area.

(dissolved H_2O, CO_2, and Cl) on glasses from this system and use these data to estimate volatile contents of primary magmas and mantle source regions.

2. Geologic Setting

[5] The Easter-Salas y Gomez Seamount Chain (hereafter ESC) is a 3000 km long east-west trending volcanic chain erupted on the interior of the Nazca Plate (Figure 1). The ESC trend intersects the east rift of the Easter microplate (hereafter EMP) at ~27°S. At least five hypotheses have been proposed to explain this linear gravity and bathymetric feature. These include a mantle hot line [*Bonatti et al.*, 1977], a leaky transform [*Herron*, 1972; *Clark and Dymond*, 1977; *Pilger and Handschumacher*, 1981; *Woods and Okal*, 1994], an incipient spreading center [*Mammerickx*, 1981], lineated zones of lithospheric extension [*Mammerickx and Sandwell*, 1986; *Sandwell et al.*, 1995], and a mantle plume located either near Easter Island [*Morgan*, 1972; *Duncan and Hargraves*, 1984; *Haase and Devey*, 1996; *Liu*, 1996] or Salas *y* Gomez Island [*Schilling et al.*, 1985; *Hanan and Schilling*, 1989; *Fontignie and Schilling*, 1991; *O'Connor et al.*, 1995; *Kingsley and Schilling*, 1998; *Naar and Wessel*, 2000]. We use the latter model, termed the mantle plume source-migrating ridge sink model (Figure 2), proposed by Schilling and coworkers [*Schilling et al.*, 1985; *Hanan and Schilling*, 1989; *Fontignie and Schilling*, 1991; *Poreda et al.*, 1993a, 1993b; *Kingsley and Schilling*, 1998]. This incorporates a numerical model that simulates mixing between a mantle plume, located near the island of Salas y Gomez, and the East Pacific Rise in the vicinity of the Easter microplate. The model predicts a focusing or channeling of upwelling buoyant, subsolidus Salas y Gomez plume (SyG) material toward the ridge as a consequence of shoaling (1.3°–3.5°) of the rheological boundary layer (i.e., the base of the lithosphere) from Salas *y* Gomez toward the east rift [*Kingsley and Schilling*, 1998]. Addition of SyG plume material to the mantle source of east rift lavas at ~27°S results in gradients in radiogenic

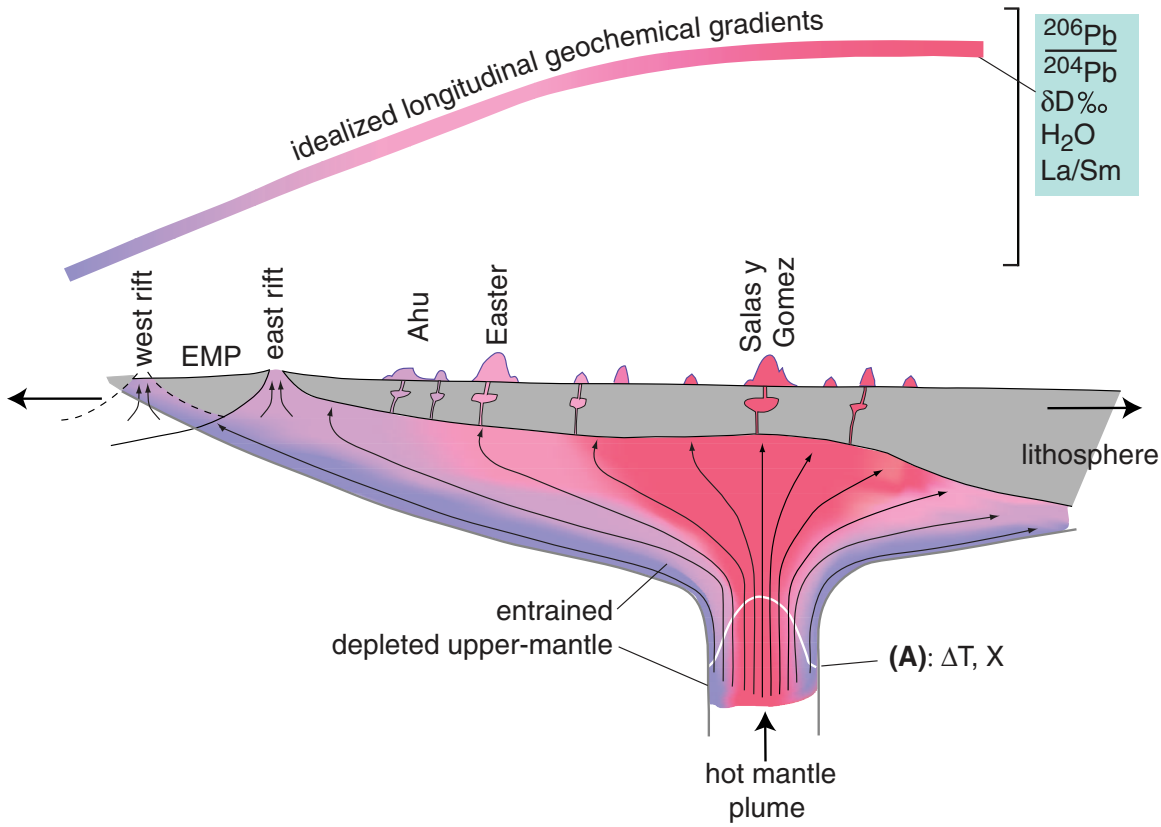

Figure 2. Model of Easter-Salas y Gomez plume [from *Kingsley et al.*, 2002]. Longitudinal cross section shows mantle plume rising underneath Salas y Gomez Island and westward mixing with depleted mantle toward the Easter Microplate along a sloping lithosphere. Binary mixing takes place in the shallow upper mantle by entrainment of depleted upper mantle (blue) with the plume source (red) enriched in incompatible and moderately incompatible trace elements, resulting in the idealized geochemical gradients. Model modified from *Kingsley and Schilling* [1998] and *Pan and Batiza* [1998].

isotopes and trace element ratios for >100 km north and south along the ridge.

[6] The SyG plume is estimated to have been active for at least the last 26 My and has left its trace from the Nazca Ridge to the current location of the east rift of the EMP (Figure 1) [*O'Connor et al.*, 1995; *Cheng et al.*, 1999]. The boundaries of the EMP include east and west rifts (propagating north and south, respectively). The plate is thought to have formed within the last 5 My with a left-stepping ridge jump on the East Pacific Rise [*Searle et al.*, 1993, 1989; *Naar and Hey*, 1991].

[7] Sample locations are listed in auxiliary material (see HTML version of the article at http://www.g-cubed.org) and shown on Figure 3. EMP samples were dredged from 25°–29°S, 113°W by the R/V *Endeavor* EN-113 cruise in 1984 [*Schilling et al.*, 1985]. ESC samples were dredged from the western ~900 km of the seamount chain (26°–27.5°S, 103°–111°W) during Legs 6 and 7 of the R/V *Melville* Gloria Expedition in 1993. Most ESC basalts west of 103°W are <1.5 Ma old (R. A. Duncan et al., manuscript in preparation, 2002). Samples are glassy pillow and flow fragments. Glass splits from the same samples have been analyzed for major elements [*Schilling et al.*, 1985; *Pan and Batiza*, 1998], trace elements [*Kingsley*, 2002], radiogenic Sr-, Nd-, and Pb-isotopes [*Hanan and Schilling*, 1989; *Fontignie and Schilling*, 1991; *Kingsley and Schilling*, 1998; *Kingsley*, 2002], C- and H-isotopes [*Kingsley et al.*, 2002], and noble gases [*Poreda et al.*, 1993a, 1993b; R. Poreda et al., manuscript in preparation, 2002]. Our H_2O,

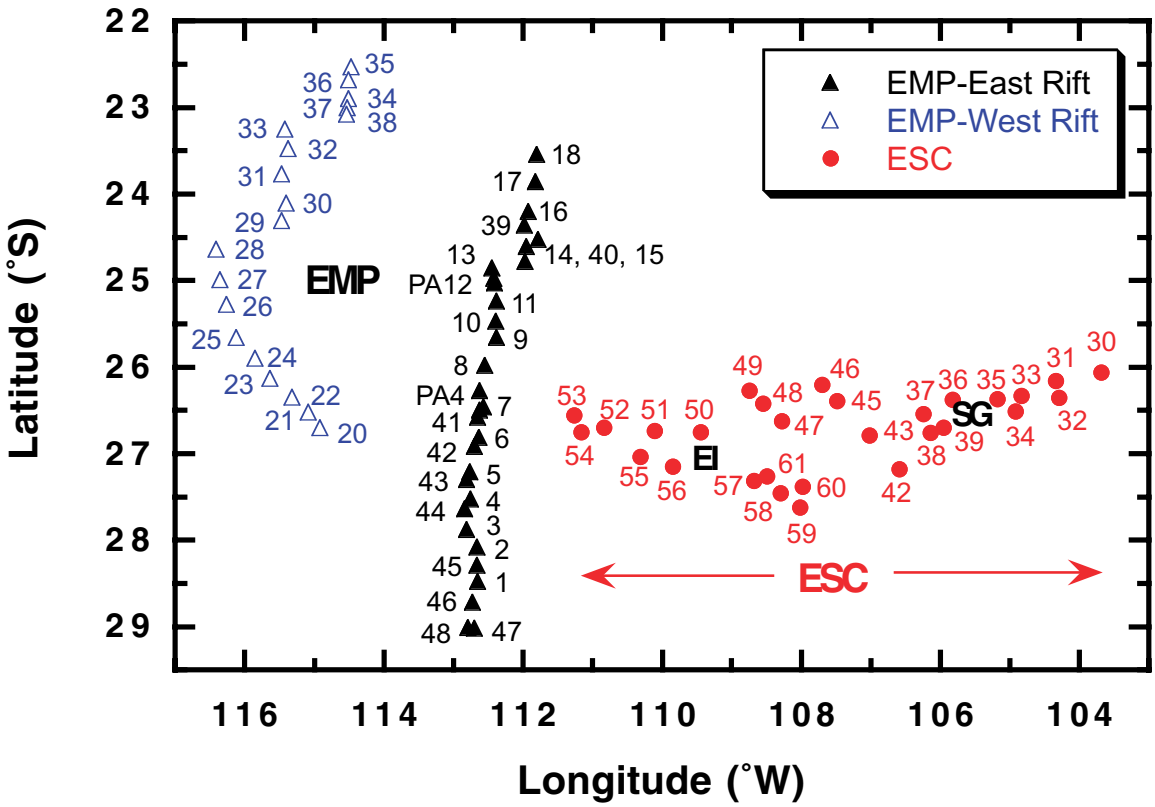

Figure 3. Dredge station map of the study area. Solid red circles (ESC) are GL07 dredges from the R/V *Melville* [*Pan and Batiza*, 1998]. Solid black triangles represent the east rift and open blue triangles represent west rift samples, both are from the EN113 R/V *Endeavor* cruise [*Schilling et al.*, 1985]. Symbols for EMP and ESC samples will remain for subsequent plots. EI is Easter Island. SG is Salas y Gomez Island.

CO_2, Cl data will be interpreted within the framework of this larger geochemical data set.

3. Methods

3.1. Infrared Spectroscopy

[8] Concentrations of dissolved water and carbon dioxide were measured using Fourier Transform Infrared Spectroscopy (FTIR) following procedures given by *Dixon and Clague* [2001]. Background correction methods, molar absorptivities, precision, and accuracy are listed in the footnote to Table 1 of auxiliary material.

3.2. Electron Microprobe

[9] Electron microprobe analysis of Cl was done in trace mode on a Cameca SX-100 microprobe at the American Museum of Natural History. An accelerating potential of 15 Kev and 45 nA beam current were used for all analyses. Count times were 60 s on peak and 30 s on background. Reported data represent an average of five spots. Natural scapolite containing 2.74 wt % Cl [*Evans et al.*, 1969] was used as the Cl standard. Precision and accuracy of Cl analyses are listed in the Table 1 (of auxiliary material) footnote. Cl detection limit is 40–50 ppm.

4. Results

[10] Results for the EMP and ESC glasses are discussed separately. Our main goal is to investigate mantle water concentrations in the sources of the EMP and ESC basalts. First we present general trends in the data (section 4.1) and discuss variations in H_2O relative to similarly incompatible elements (section 4.2). Next we identify samples whose volatile concentrations have been modified by degassing (section 4.3) or assimilation of brine (section 4.4) or serpentinite (section 4.5). Finally, we discuss water concentrations in parental magmas (section 5.1), primary magmas (section 5.2), and mantle

end-members (section 5.3) using samples unmodified by these degassing and assimilation processes.

4.1. Concentrations of H_2O, CO_2, and Cl

[11] Major, trace and volatile element concentrations for 32 EMP glasses and 34 ESC glasses are listed in auxiliary material.

4.1.1. H_2O, CO_2, and Cl in EMP glasses

[12] EMP glasses have 0.07–0.76 wt % H_2O, 70–347 ppm CO_2, and 12–2640 ppm Cl (Table 1 of auxiliary material). H_2O concentrations in EMP glasses are highest at 27°S latitude (Figure 4a), where the plume channel joins the east rift of the microplate, and decrease to the north and south. Cl concentrations in east rift glasses are scattered, with maximum values just north of the entrance of the plume channel (~25°S). Cl concentrations in west rift glasses are more uniform (mostly below 300 ppm) with maximum values at 23.5°S (Figure 4b). CO_2 concentrations do not correlate with location or depth of eruption (Figure 4c).

4.1.2. H_2O, CO_2, and Cl in ESC glasses

[13] ESC glasses have 0.29–1.55 wt % H_2O, 0–213 ppm CO_2, and 30–1109 ppm Cl (Table 2 of auxiliary material). On average, ESC glasses have higher H_2O and Cl than EMP glasses at the same MgO content, consistent with previous studies of plume-related basalts, such as the Azores [*Schilling et al.*, 1980, 1983; *Kingsley and Schilling*, 1995] and Hawaii [*Garcia et al.*, 1989; *Dixon et al.*, 1997; *Wallace*, 1998; *Wallace and Anderson*, 1998; *Dixon and Clague*, 2001]. Concentrations of H_2O and Cl increase away from the east rift of the microplate toward the island of Salas *y* Gomez (Figures 5a and 5b) consistent with spatial variations of other incompatible elements [*Kingsley and Schilling*, 1998]. CO_2 concentrations correlate negatively with water and chlorine. The lowest concentrations occur near Salas y Gomez and increase toward the microplate (Figure 5c).

4.2. Comparison of H_2O to Other Incompatible Elements

[14] Variations in water concentrations are often evaluated using ratios of water to similarly incom-

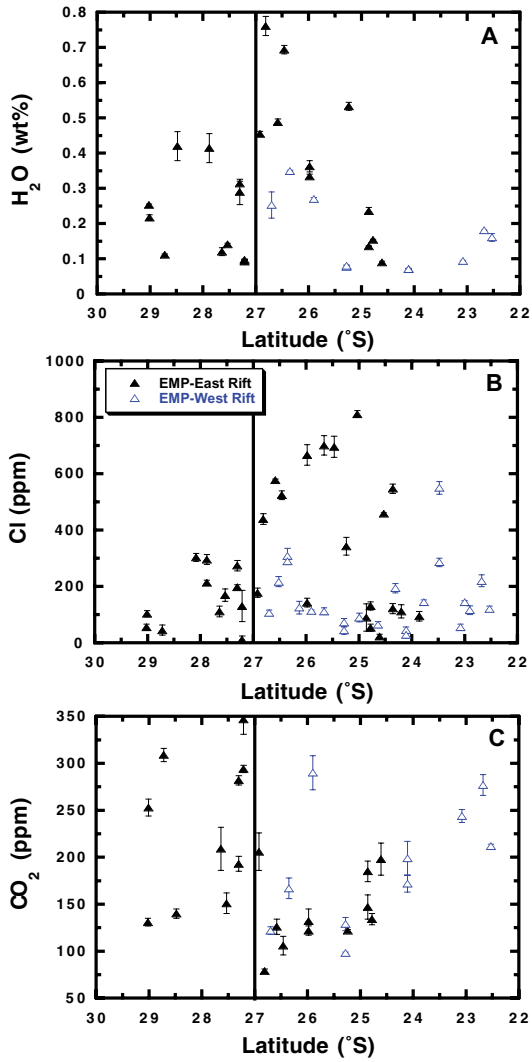

Figure 4. (a) H_2O concentrations (wt %) for the EMP are divided into east and west rifts and plotted versus latitude (north is right, south is left). Concentration range from normal MORB values (> 0.1–0.4 wt %) to higher concentration, plume-influenced values of 0.8 wt %, with the highest concentrations near the entry of the plume channel (solid line) at 27°S. Concentrations decline north and south of that latitude. (b) Cl concentrations (ppm) for the EMP are plotted versus latitude and show that the maximum in Cl concentration (25°S) does not coincide with the entry of the plume channel (black line). Concentrations decline north and south of 25°S. (c) CO_2 concentrations (ppm) versus latitude for the EMP shows that CO_2 concentrations reach a minimum at 27°S and increase north of that latitude. South of the plume channel CO_2 concentrations are scattered and do not vary systematically with depth. Errors shown for H_2O, Cl, and CO_2 are 1σ standard deviation of mean. Sample 45D-1 at 28.29°S has 2640 ppm Cl and is not shown.

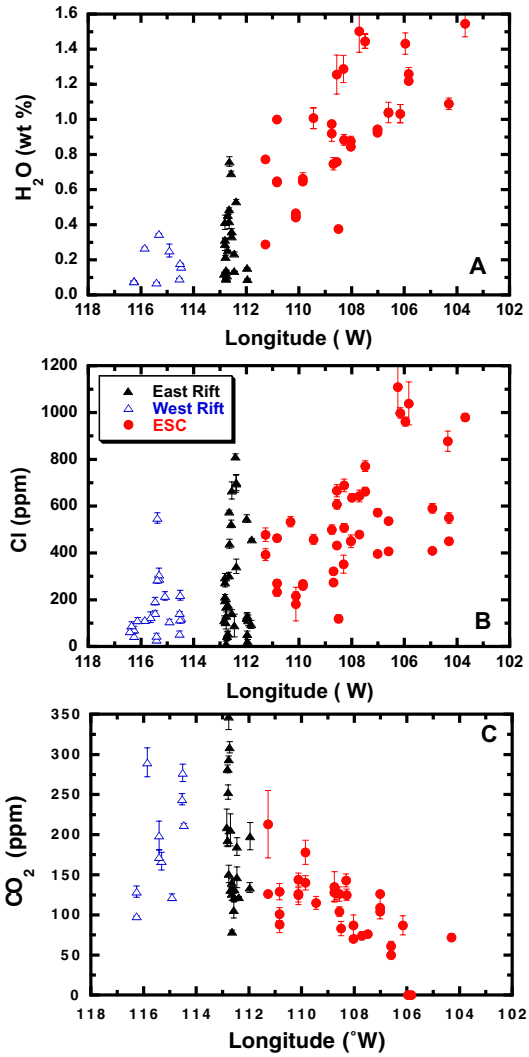

Figure 5. (a) H_2O concentrations (wt %) plotted versus longitude (east is right, west is left) for ESC and EMP samples. Water concentrations for the seamounts are higher than those for the microplate, and increase away from the east rift of the EMP, with maximum concentrations near the island of Salas y Gomez. (b) Cl concentrations (ppm) plotted against longitude for EMP and ESC samples. Concentrations of Cl are higher for the seamounts than the microplate, with a maximum near the island of Salas y Gomez. (c) CO_2 concentrations (ppm) plotted versus longitude for EMP and ESC samples. This pattern of enrichment is opposite to that of Cl and H_2O, with the highest concentrations occurring on the east rift of the EMP, and the lowest concentration near the island of Salas y Gomez. Errors are same as in Figure 4.

patible nonvolatile oxides (i.e., K_2O and P_2O_5) or trace elements (i.e., La and Ce), where the order of relative incompatibility during fractional crystallization and partial melting is $K_2O > La \approx H_2O > Ce > P_2O_5$ [e.g., *Dixon et al.*, 1988, 1991, 1997; *Michael*, 1988, 1995; *Garcia et al.*, 1989; *Jambon and Zimmerman*, 1990; *Clague et al.*, 1995; *Danyushchevsky et al.*, 2000; *Simons*, 2000; *Dixon and Clague*, 2001]. Given that water behaves similarly to the light rare earth elements (LREE), incompatible element-enriched basalts (e.g., plume basalts) derived from more fertile source regions are expected to have higher H_2O concentrations than MORB. Because water is more incompatible than Ce, we expect H_2O/Ce to increase slightly as the source becomes more enriched in incompatible elements (rare earth patterns become more LREE-enriched) [*Danyuschevsky et al.*, 2000; *Dixon and Clague*, 2001]. We prefer to use Ce as our index element, because (1) recent work has shown significant variation in H_2O/K_2O in oceanic basalts due to larger heterogeneity in K in different mantle source regions [*Sobolev and Chaussidon*, 1996; *Danyushchevsky et al.*, 2000; *Simons*, 2000; *Dixon and Clague*, 2001] and (2) H_2O/Ce should correlate positively with other indicators of source region enrichment (i.e., La/Sm or K/Ti). Thus, when enrichments in water are coupled with La and Ce in plume basalts, the simplest explanation for the higher water concentrations is a less depleted source, not an additional hydrous component. Conversely, decoupling of H_2O from La and Ce in plume basalts would require more complex processes, including involvement and possible migration into or out of the mantle plume of a separate C+H+O fluid phase, addition of hydrated or dehydrated recycled crustal components into the source, or shallow level processes such as assimilation or degassing.

4.2.1. H_2O/Ce in EMP basalts

[15] Water correlates positively with Ce in the EMP glasses (Figure 6a). A linear regression through the data yields $H_2O = -0.039 + 0.021 * Ce$ with $R^2 = 0.983$. The H_2O/Ce ratio along the best-fit line ranges from ~145 at 10 ppm Ce to ~210 at 35 ppm Ce. High H_2O/Ce ratios (210 ± 20) occur in incompatible element-enriched samples on the east rift near the entry of the plume channel (EN113-6D-1, 7D-1, 11D-10, 41D-1, 42D-1, and 8D-13); whereas low H_2O/Ce ratios (150 ± 10) occur in

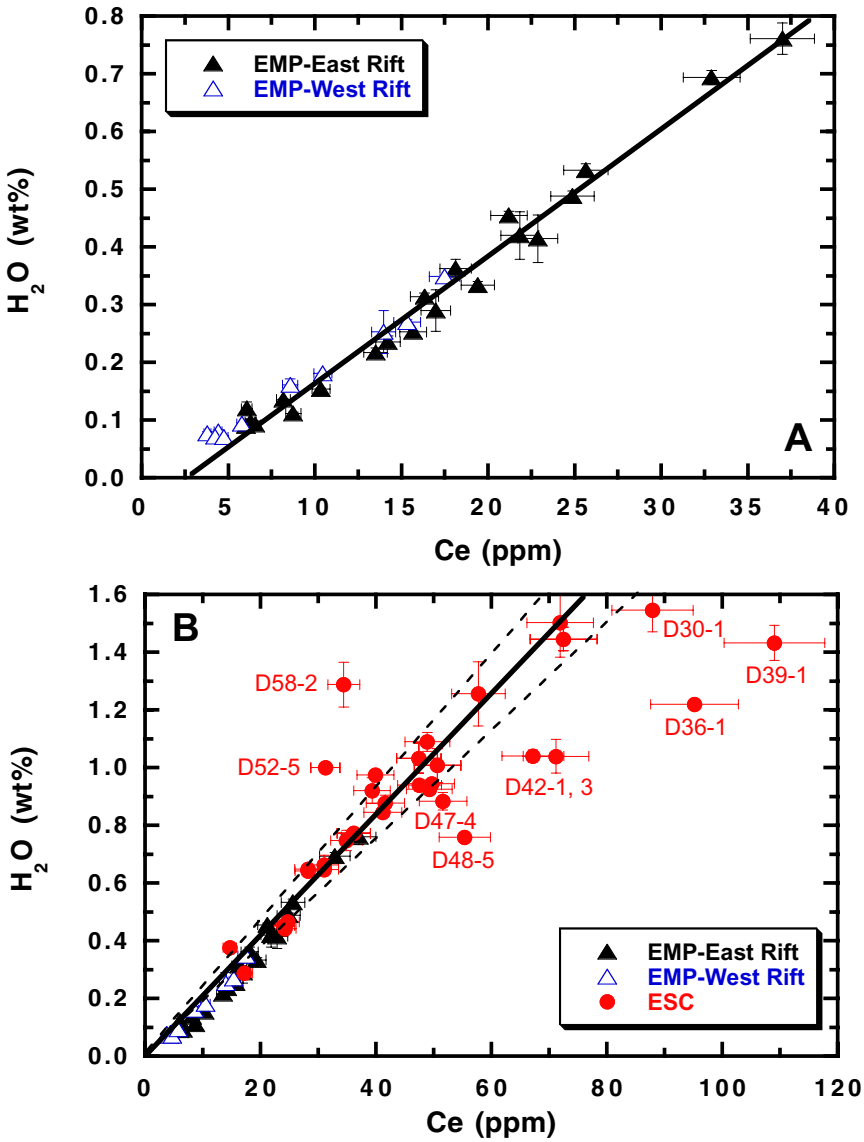

Figure 6. (a) H_2O (wt %) plotted against Ce (ppm) for EMP samples. Line is best fit through East Rift data. (b) H_2O (wt %) versus Ce (ppm) for EMP and ESC glasses. Solid line is H_2O/Ce line = 210, two dashed lines show 10% deviation from solid line (H_2O/Ce = 190 and 230). Two ESC samples are significantly above the line, and eight are below. (Sample 36–3 is within uncertainty of 36–1 and was unintentionally omitted.) Error bars for H_2O concentrations are 1σ standard deviation from mean and for Ce concentrations are ±8% of the amount present.

incompatible element-depleted EMP samples (EN113- 5D-1, 5D-10, 14D-1, 30D-1, 38D-1, 40D-1, and 46D-2) far from the plume channel. Though the mean H_2O/Ce of all EMP basalts (175 ± 23) is essentially identical to the Pacific average (184 ± 41 [*Michael*, 1995]), we believe a value of 150 ± 10 is a better estimate for depleted Pacific MORB because the affect of plume-influenced samples has been removed. For example, samples from cruise GS7202 (Pacific-Nazca Ridge ~28°S) were incorporated into the Pacific MORB average, even though they are near the location of the entrance of the Easter plume channel and hence have higher H_2O/Ce.

[16] Five strongly depleted samples (EN113- 26D-1, 26D-10, 30D-1, 35D-1, and 44D-5), however, have anomalously high H_2O/Ce ratios for their Ce content (Figure 7). These are some of the most depleted samples from the EMP, both in terms of

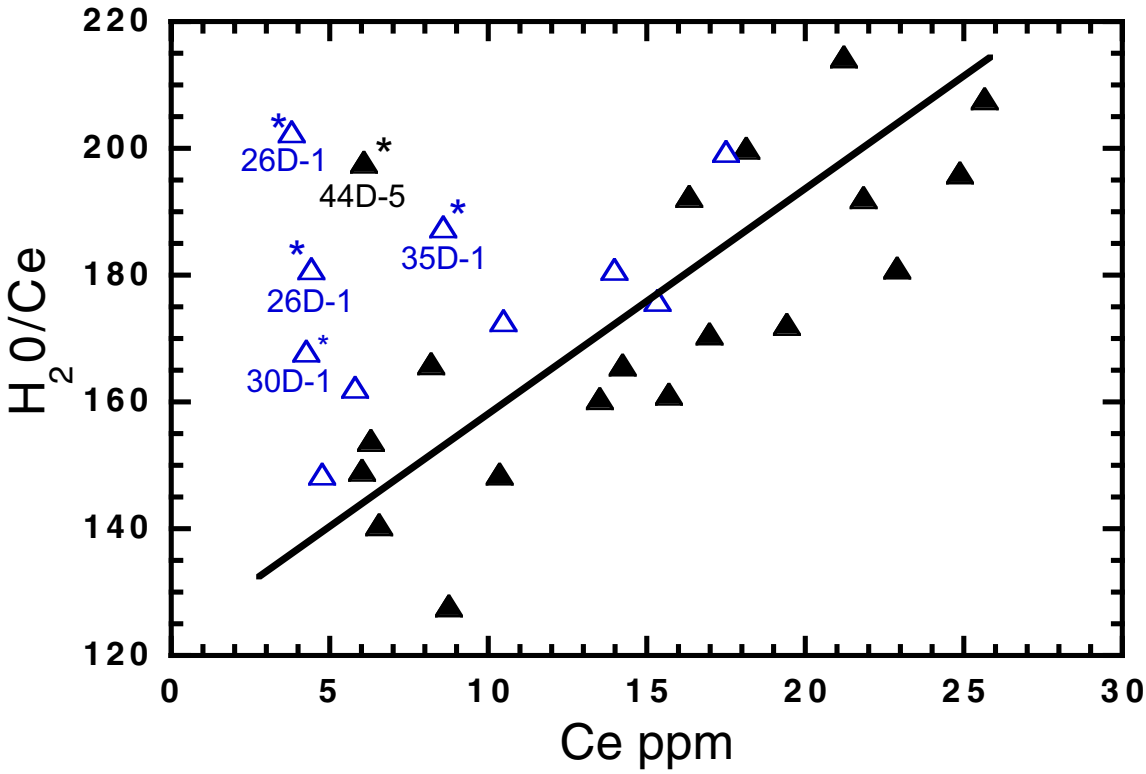

Figure 7. H_2O/Ce shows a positive correlation with Ce concentration (ppm) for EMP samples. This trend in H_2O/Ce reflects mixing between the higher H_2O/Ce of the plume and the lower H_2O/Ce of the MORB mantle source. Several depleted EMP samples (EN113- 26D-1, 26D-10, D30-1, 35D-1, and 44D-5) have H_2O/Ce ratios much higher than the rest of the EMP samples at the same Ce concentration. These samples will be marked with an asterisk in subsequent plots.

trace elements and radiogenic isotopes. The high H_2O/Ce ratios in these samples may be related to small amounts of assimilation of a seawater-derived component, discussed in section 4.4.

4.2.2. H_2O/Ce in ESC basalts

[17] Water concentrations in ESC glasses with <0.80 wt % H_2O correlate linearly with Ce and are colinear with the microplate samples (Figure 6b). Above 0.8 wt %, H_2O, the data are more scattered. The majority of the seamount samples (69%) have H_2O/Ce of 210 ± 20 (±10%) consistent with H_2O/Ce observed in the plume-influenced EMP basalts. Ten seamount glasses have H_2O/Ce more than 10% from a value of 210 (Figure 6b); eight samples (GL07- D30-1, D36-1, D36-3, D39-1, D42-1, D42-3, D47-4, and D48-5) have lower H_2O/Ce and two (GLO7- D52-5, D58-2) have higher H_2O/Ce.

[18] Low H_2O/Ce ratios are most likely caused by degassing of water (section 4.3). High H_2O/Ce may be the result of (1) assimilation of Cl-rich seawater or hydrothermal brine into the magma (shallow assimilation [e.g., *Michael and Cornell*, 1998]), (2) assimilation of hydrated crust or upper mantle (shallow assimilation [e.g., *Nielsen et al.*, 2000]), or (3) incorporation of a hydrous recycled crustal component in the source region. In section 4.5, we use Cl data to distinguish hypothesis 1 from hypotheses 2 and 3.

4.3. Degassing

[19] In order to evaluate the extent of low pressure degassing of water, we estimate bulk water (measured water dissolved in the glass plus estimated water in vesicle gas) for comparison to measured dissolved water (Tables 1 and 2 of auxiliary material). If significant amounts of water are present in vesicles, then estimated bulk water will be greater than measured dissolved water. Bulk water contents are calculated based on (1) vesicularity, (2) calculated vapor

composition at the pressure of vapor saturation (P_{equil}) [*Dixon*, 1997], (3) ideal gas behavior for the vesicle gases, and (4) a "rigid temperature" of 1000°C [*Moore et al.*, 1977]. Vapor composition is expressed in terms of mole fraction water in a CO_2 + H_2O vapor ($X^v_{H_2O}$). These provide minimum estimates of preeruptive magmatic water concentrations because some bubbles may have escaped the system [e.g., *Moore et al.*, 1977; *Pineau and Javoy*, 1983; *Des Marais and Moore*, 1984; *Gerlach*, 1991; *Graham and Sarda*, 1991]. In doing these calculations, we assume that collection depth is equivalent to eruption depth and that P_{erupt} = (eruption depth in m)/10. Glasses having $P_{equil} > P_{erupt}$ are supersaturated with respect to a CO_2-H_2O vapor at their depth of eruption. Glasses having $P_{equil} = P_{erupt}$ are vapor-saturated at their depth of eruption. Water-poor MORB tend to be supersaturated, indicating that the kinetics of bubble nucleation and growth, driven by exsolution of CO_2, are too slow to maintain melt-vapor equilibrium during magma ascent [*Fine and Stolper*, 1986; *Stolper and Holloway*, 1988; *Dixon et al.*, 1988, 1995]. In a suite of basalts erupted over a limited depth range, dissolved H_2O and CO_2 should correlate negatively if vapor saturation is maintained to the eruption depth [*Dixon and Stolper*, 1995], but that correlation will be smeared out if vapor saturation is arrested at various depths during ascent. In general, water loss is not likely from EMP glasses because they are erupted deep (> 2050 m), have low volatile contents, and have low vesicularities (0–10 vol %), whereas water loss may be more likely from ESC glasses because they are erupted over a wider range of depths (3268–1814 m), have higher volatile contents, and have a wider range of vesicularities (0–30 vol %).

4.3.1. Degassing of EMP basalts

[20] Calculated P_{equil} values for EMP glasses are greater than or equal to P_{erupt} (Figure 8). This indicates that most EMP glasses are supersaturated with respect to a CO_2 + H_2O vapor, consistent with previous results for MORB. The poor correlation between dissolved H_2O and CO_2 concentrations in EMP basalts reflects the wide range of P_{equil}. The low vesicularity of EMP lavas combined with the CO_2-rich composition of the vapor phase ($X^v_{H_2O}$ ranges from 0.00 to 0.09) results in calculated bulk water within analytical error of the dissolved water concentrations (<2.5% of their initial water in the vapor phase). Thus all EMP glasses have lost significant CO_2 during low pressure degassing but none have lost significant H_2O.

4.3.2. Degassing of ESC basalts

[21] In contrast, most (94%) ESC glasses have P_{equil} values that are equivalent within uncertainty to P_{erupt}, indicating that they are saturated with respect to a CO_2 + H_2O vapor phase for their depth of eruption (Figure 8). Also, the range of P_{equil} values at a given eruption depth is smaller for ESC samples than for EMP samples. The negative correlation of dissolved H_2O and CO_2 in ESC glasses is consistent with their being vapor saturated at the depth of eruption. The greater proportion of vapor-saturated samples in the seamount suite may be related to more rapid vapor-melt equilibration rates in water-rich melts (>0.4 wt % H_2O) than in typical MORB melts (<0.4 wt % H_2O), perhaps related to faster diffusion rates of H_2O and CO_2 in hydrous melts, combined with shorter diffusive path lengths for samples with greater vesicularity [*Dixon et al.*, 1997].

[22] When calculated bulk water concentrations are compared to measured dissolved water concentrations, three groups of samples can be defined (Figure 9). Samples in the first group (GL07- D36-1, D36-3, and D42-1) are extensively degassed, having lost ~20% of their initial H_2O to the vapor phase. These samples have vesicularities greater than 25 vol %, $X^v_{H_2O}$ between 0.52 and 0.87, and glass that is partially devitrified. In general, the extensively degassed samples are fractionated (<6 wt % MgO) and are erupted at shallow seafloor depths (<2000 m). Samples in the second group (GL07- D32-4, D39-1, D42-3, D43-1, D43-2, D46-2, and D47-4) are moderately degassed and have lost 5–10% of their initial dissolved H_2O to bubbles. These glasses have lower vesicularities (7–10 vol %) and have less water-rich vapor compositions ($X^v_{H_2O}$ = 0.30

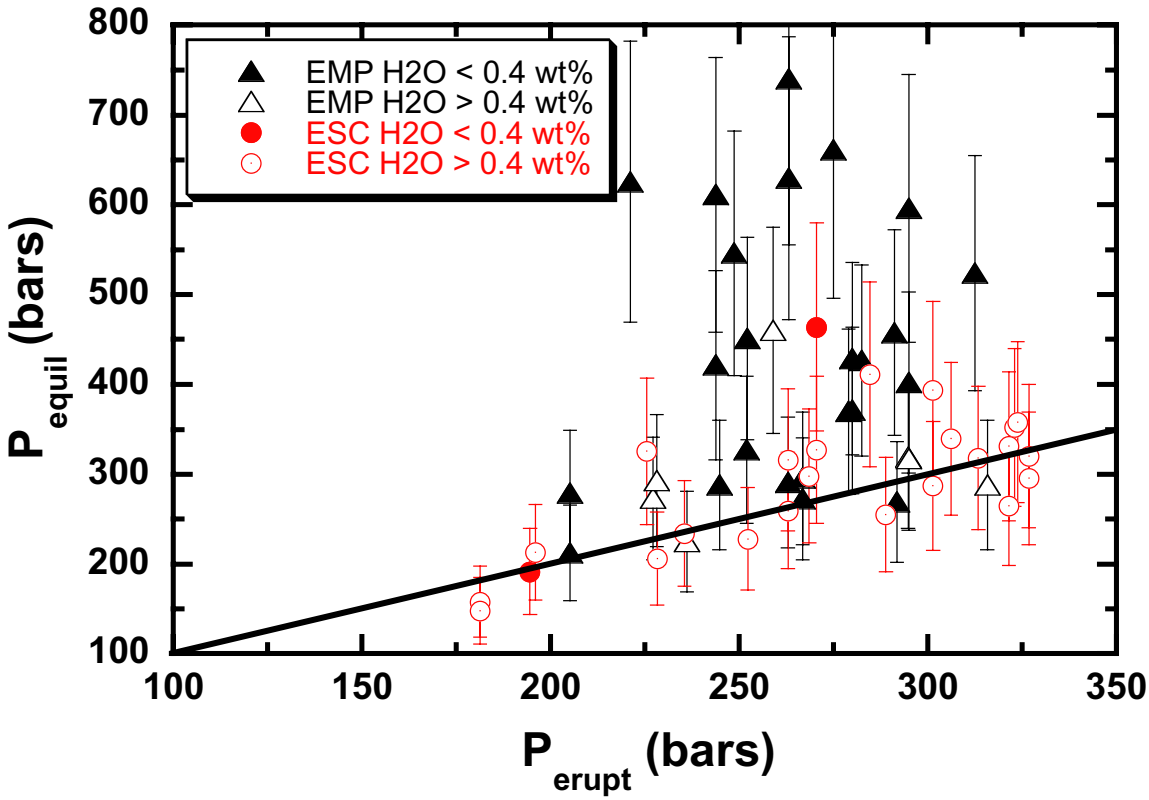

Figure 8. Vapor saturation pressures [*Dixon*, 1997] plotted versus collection depth for EMP and ESC glasses, divided into samples with total H_2O above 0.4 wt % and samples with less than 0.4 wt % H_2O. Shallowest depths of collection are ~1800 m for the seamount samples. Samples plotting within uncertainty of the 1:1 line are saturated with a CO_2-H_2O vapor phase at the pressure of collection. The majority of EMP samples are supersaturated for their depth of eruption, with a wide range of equilibration pressures. The majority of ESC samples are saturated for their depth of eruption, with a smaller range in pressure of equilibration. These features are common to MORB and seamount lavas and are related to the kinetics of nucleation and bubble growth.

to 0.87) than the extensively degassed samples. The remaining ESC samples have vesicularities <7% and have lost negligible amounts (<5%) of dissolved H_2O to the vapor phase.

[23] In general, the samples identified as having lost water based on bulk volatile analysis are also the ones with low H_2O/Ce, supporting our hypothesis that the low H_2O/Ce ratios result from degassing. Only two low H_2O/Ce samples (GL07- D30-1, and D48-5) were not identified as having lost water by bulk volatile analysis. CO_2 was not analyzed in D30-1 because of noise in the carbonate region, therefore bulk water could not be calculated. The disagreement between the two techniques for sample D48-5 is probably related to uncertainties in vesicularity estimates caused by sample heterogeneity or bubble loss during flow. We therefore assume that a total of 12 samples (10 samples identified by bulk volatiles plus D30-1 and D48-5) have lost water due to eruptive degassing. These samples will not be included in the calculation of parental magma and mantle source water concentrations.

4.4. Assimilation of a Cl-Rich, Seawater-Derived Component

[24] Chlorine behaves as an incompatible element during melting and crystallization, with an incompatibility in mantle minerals similar to K and greater than La [*Schilling et al.*, 1980; *Sun*, 1982; *McDonough and Sun*, 1995]. However, recent studies have shown that Cl concentrations in oceanic basalts are easily modified by assimilation of Cl-rich, hydrothermally influenced material.

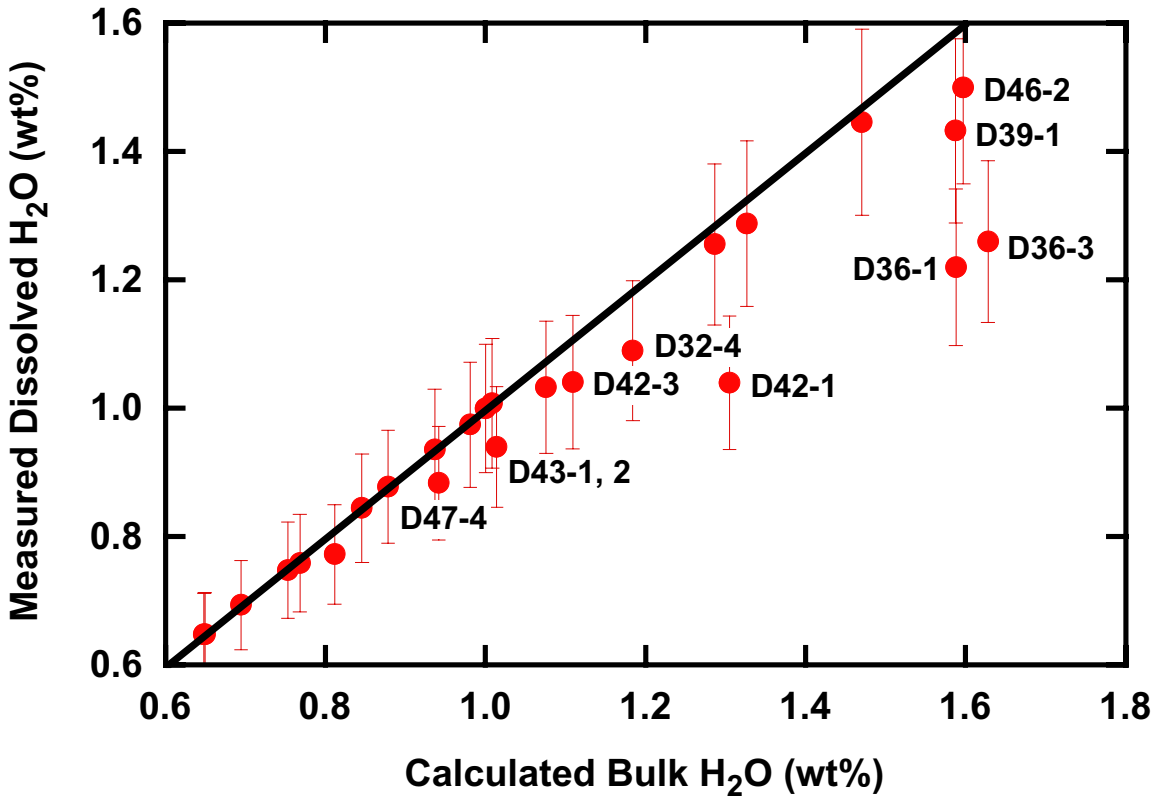

Figure 9. Dissolved total H_2O (wt %) plotted against calculated bulk H_2O (wt %) (volatiles in glass plus vesicles) for the ESC only. Ten samples (GL07- D32-4, D36-1, D36-3, D39-1, D47-4, D43-2, D46-2, D42-1, D42-3, D43-1) are more than 10% off the 1:1 line, and are thought to have degassed water.

MORBs on fast spreading ridges are often enriched in Cl, relative to those erupted along slowly spreading ridges [*Michael and Schilling*, 1989; *Jambon et al.*, 1995; *Michael and Cornell*, 1998; *Kent et al.*, 1999a, 1999b; *Dixon and Clague*, 2001]. This may be related to the almost constant shallow melt lens and hydrothermal systems beneath fast spreading ridges, compared to the intermittent melt lens and hydrothermal activity at slow spreading ridges [*Sinton and Detrick*, 1992]. Below we investigate evidence for Cl assimilation in EMP and ESC basalts.

4.4.1. Evidence for assimilation of Cl-rich component in EMP basalts

[25] Cl concentrations in EMP glasses are decoupled from other incompatible elements and exhibit a wide range of values at a given K_2O or La content (Figure 10a). The location of highest Cl concentrations in the EMP glasses does not coincide with the entry of the plume channel, therefore the high Cl concentrations are not related to plume input. Differentiated samples (MgO < 7%) have higher Cl concentrations than relatively undifferentiated samples (Figure 11), consistent with the idea that magmas that reside and crystallize in shallow magma chambers have greater opportunity to assimilate Cl-rich materials [*Michael and Cornell*, 1998]. Thus the dominant control of the Cl concentrations in EMP basalts is assimilation of a Cl-rich, hydrothermally derived component.

[26] Cl concentrations in four EMP glasses (EN113- 8D-13, 14D-10, 40D-1, and 42D-1) are the lowest at a given MgO and correlate positively with La (Cl/La = 17 ± 5) (Figure 10a), suggesting that these four samples represent uncontaminated magma. Because of lack of evidence for degassing of water from EMP glasses, it is unlikely that their low Cl concentrations are related to degassing

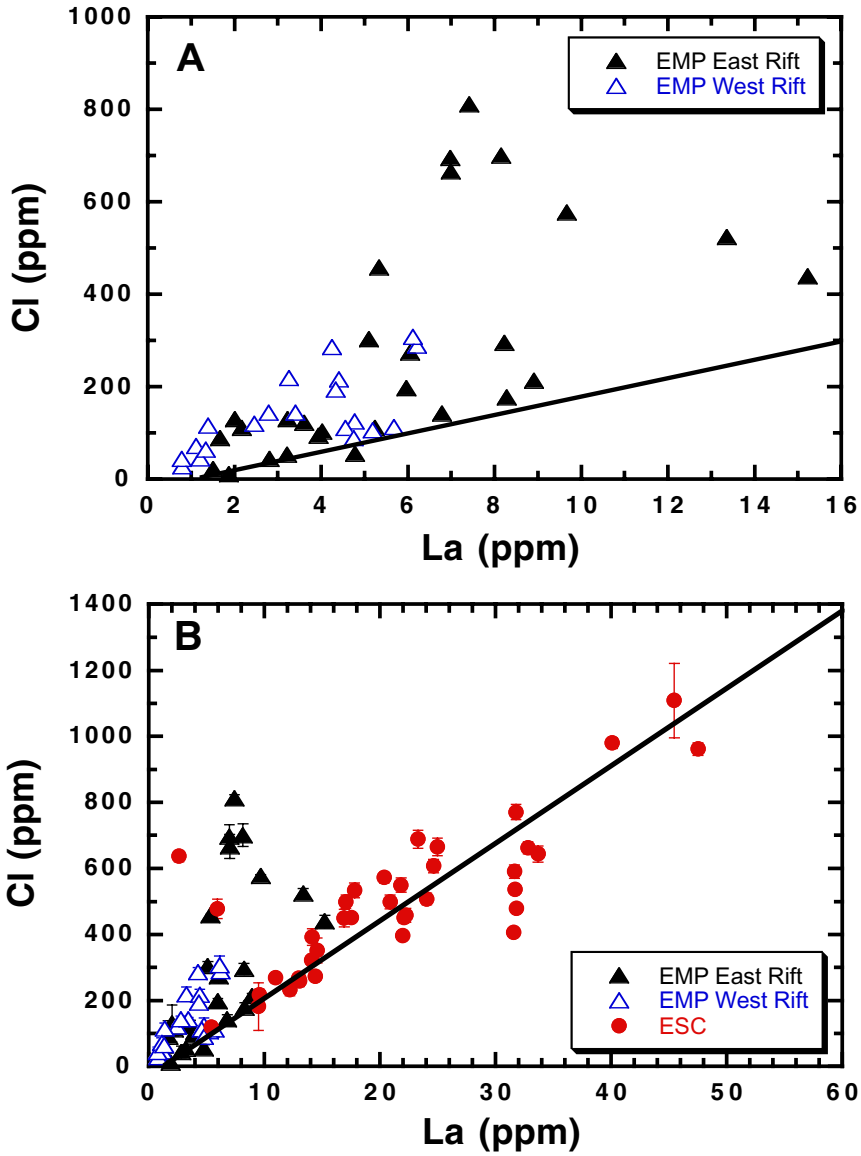

Figure 10. (a) Cl versus La for the east and west rifts of the microplate. Decoupling of Cl from La suggests that many EMP samples may have been affected by shallow assimilation of a Cl-rich hydrothermal component. The lowest Cl for a given La defines a Cl/La line of 17 ± 5. (b) Cl versus La for EMP and ESC data. Most of the ESC data are within 20% of a Cl/La line of 23 ± 5.

[*Webster et al.*, 1999]. These samples will be used to estimate mantle Cl concentrations (section 5.3).

4.4.2. Lack of evidence for assimilation of Cl-rich component in ESC basalts

[27] In contrast to the EMP samples, chlorine concentrations in ESC glasses vary roughly linearly with other similarly incompatible elements, like K and La. A plot of Cl versus La for all EMP-ESC glasses (Figure 10b) has a best fit line through the data that intersects the La axis, implying that Cl is more incompatible than La, consistent with *Schilling et al.* [1980]. A Cl/La ratio of ~23 ± 5 fits the majority (81%) of the ESC data. Only two samples (GL07 D53-5 and D60-1) have significantly higher Cl/La and have likely assimilated a Cl-rich component. These are also the two most depleted ESC samples; consequently small amounts of assimilation are likely to have a large effect on Cl/La. The

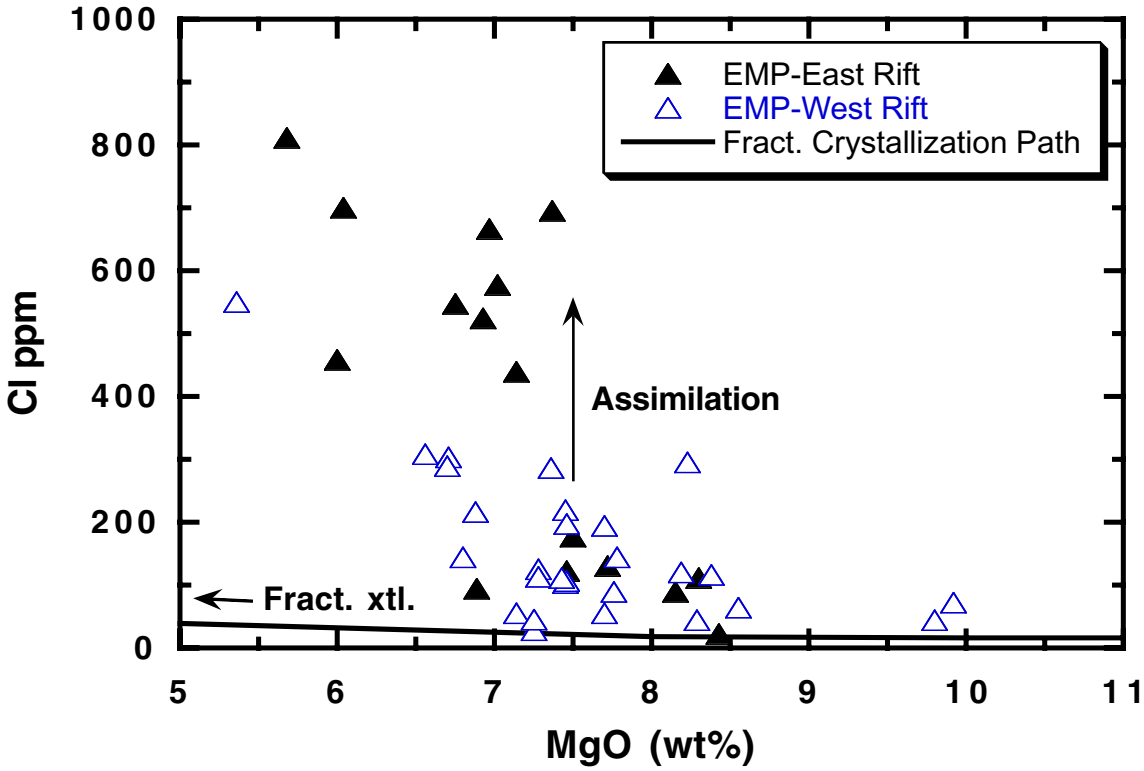

Figure 11. A correlation between Cl and MgO suggests that more differentiated samples (MgO < 7 wt %) are more likely to assimilate Cl-contaminated material because of longer residence times in shallow crustal magma chambers. Solid line is fractional crystallization path for depleted EMP compositions.

relatively constant Cl/La ratios in most ESC glasses suggest that Cl concentrations are controlled mainly by magmatic processes (mantle source composition and extents of melting and differentiation) with only minor modification by assimilation.

4.4.3. Evidence for limited assimilation of H_2O in EMP basalts

[28] A positive correlation between H_2O/Ce and Cl/La in a few depleted ($[La/Sm]_n$ < 0.9) EMP glasses (Figure 12) suggests that assimilation of a Cl-rich component also affected the H_2O concentrations. The five samples with anomalously high H_2O/Ce for their Ce content (EN113- 26D-1, 26D-10, 30D-1, 35D-1, and 44D-5) also have the highest Cl/La, consistent with assimilation as a common cause. Assuming initial H_2O/Ce and Cl/La ratios of ~150 and ~17, respectively, assimilation resulted in addition of ~150 to 400 ppm H_2O for five samples, and ~20 to 2600 ppm Cl for the great majority of the samples. The calculated H_2O/Cl of the assimilant is 3.8, consistent with a 35–40% brine [*Kent et al.*, 1999b]. Although Cl concentrations in oceanic basalts are commonly modified by assimilation, H_2O concentrations commonly are not [*Michael and Schilling*, 1989; *Michael and Cornell*, 1998; *Michael*, 1995; *Kent et al.*, 1999a, 1999b; *Dixon and Clague*, 2001]. We believe H_2O contamination in the 5 EMP samples is detectable because they are depleted overall in incompatible trace elements; therefore small additions of H_2O for these samples have large effects on ratios of H_2O to incompatible elements. This may be the first clearly documented evidence of small-scale assimilation of H_2O on mid-ocean ridges due to hydrothermal circulation.

4.4.4. Lack of evidence for assimilation of H_2O in most ESC basalts

[29] In contrast to the depleted EMP samples, there is no correlation between H_2O/Ce and Cl/La in the seamount samples. The two ESC glasses (GL07

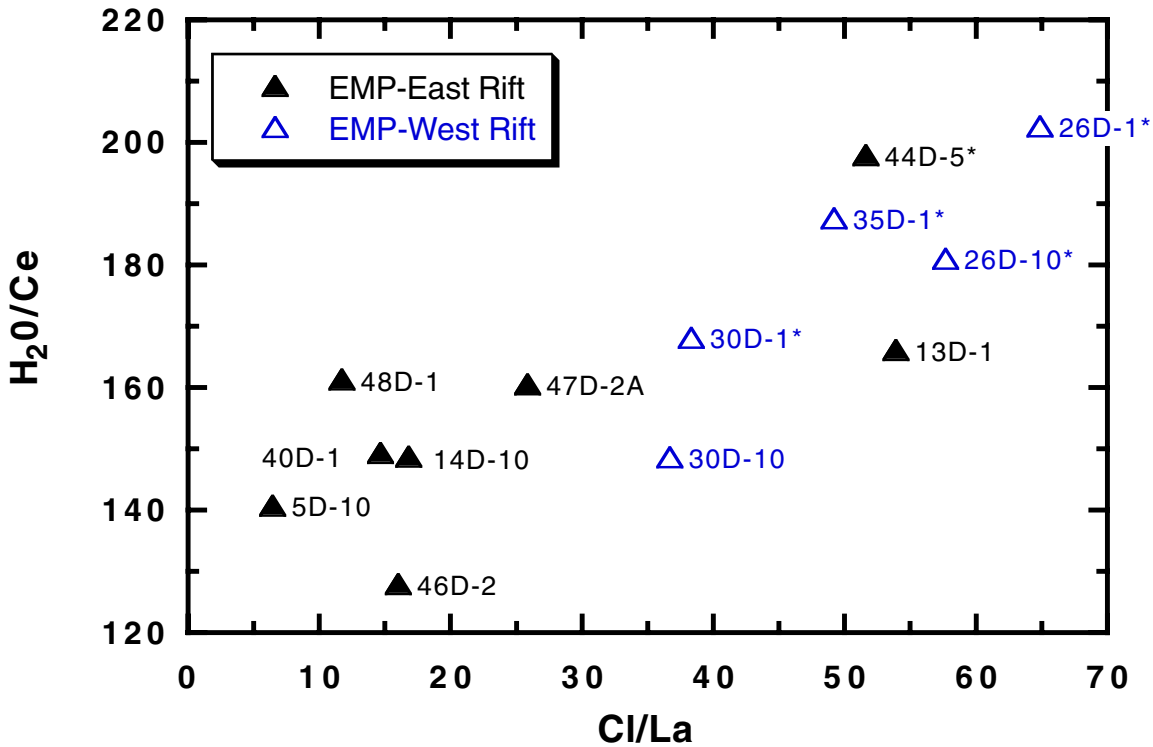

Figure 12. H_2O/Ce versus Cl/La EMP samples filtered to show only samples with minimal plume influence ((La/Sm)$_n$ < 0.9). The positive correlation between H_2O/Ce and Cl/La for non-plume-influenced EMP samples suggests assimilation of H_2O along with Cl. Glasses marked with an asterisk have high H_2O/Ce at a given Ce (Figure 7).

D58-2 and D52-5) with anomalously high H_2O/Ce ratios, requiring excess H_2O concentrations of ~0.57 wt % and ~0.34 wt %, respectively, are not enriched in Cl. Therefore it is unlikely that the high water concentrations are caused by assimilation of a Cl-rich, hydrothermal component as proposed for the ridge crest samples. This is not surprising. Assimilation of a Cl-rich component is rare at slowly spreading ridges [e.g., *Michael and Cornell*, 1998], and it is unlikely that long-lived hydrothermal systems capable of producing Cl-rich brines could be sustained at these small seamounts.

4.5. Origin of Anomalously High H_2O ESC Samples by Assimilation of Serpentinite

[30] The absence of excess Cl concentrations in the two high H_2O ESC samples rules out assimilation of a Cl-rich brine (hypothesis 1) but does not rule out shallow level assimilation (hypothesis 2). These samples are not anomalous in any way, including D/H ratios [*Kingsley et al.* , 2002], other than their high water concentrations. The fact that their D/H ratios are consistent with the regional gradient precludes assimilation of seawater, which would result in significantly heavier δD values. It may be that in slowly spreading environments or off-axis seamounts the assimilant is hydrated ultramafic or mafic rocks, instead of hydrothermal brines. Glasses with anomalously high H_2O contents and no Cl enrichment have also been described from Lamont seamounts [*Danyushevsky et al.*, 2000]. Because serpentinized harzburgites are so depleted in incompatible trace elements, assimilation into basaltic melt, in particular enriched basaltic melts, would have little effect except for H_2O concentrations and possibly Sr-isotopes. Assimilation of ~3–5% serpentine with ~13% H_2O would result in the excess water concentrations observed in the two high H_2O ESC glasses. Assimilation might even go undetected by stable isotopic data, given the overlap in δD_{VSMOW} for the seamount samples (−36 to −63‰ [*Kingsley et al.*, 2002] and serpentinized

peridotites (−30 to −85‰ [*Sheppard and Epstein*, 1970; *Wenner and Taylor*, 1973; *Stakes and O'Neil*, 1982; *Agrinier et al.*, 1995]). Sr-isotopic ratios in serpentinized harzburgites should be higher than those in depleted MORB, though they may be similar in this region because the few million year old oceanic crust in this region has been influenced by the SyG mantle plume [*Hanan and Schilling*, 1989; *Fontignie and Schilling*, 1991; *Kingsley and Schilling*, 1998]. We cannot rule out the possibility that a hydrous assimilant occurs as separate hydrous mantle component (hypothesis 3), but note that if the hydrous component is mantle-derived, it must be present in extremely small and isolated amounts. We favor a model of crustal assimilation of serpentinized harzburgites for the high water samples because it is difficult to explain how isolated hydrous mantle components could make it so far along the plume channel (almost to the ridge) without melting or diluting their high water signature by mixing along the way.

5. Discussion

5.1. Parental Magma Concentrations

5.1.1. Coupling of H_2O, Cl, and nonvolatile trace element concentrations

[31] Primitive-mantle-normalized trace element concentrations corrected for shallow fractionation to a constant value of MgO = 8.0 wt % ($Ce_{8.0}$, $(H_2O)_{8.0}$, $La_{8.0}$, $K_{8.0}$ and $Cl_{8.0}$) for representative EMP and ESC glasses are shown in Figures 13a–13c. Hereafter, we refer to melt compositions corrected to MgO = 8.0 wt % as parental magmas. Samples that have degassed or assimilated water are omitted. Primitive-mantle concentrations are listed in the caption to Figure 13. Fractionation correction methods are listed in the caption to Table 1.

[32] EMP parental magma compositions (Figure 13a) are shown as a function of distance from the entry of the plume channel (27°S), where sample EN113 6D-1 is closest and EN113 48D-1 is farthest along the east rift. EMP samples have normalized $(H_2O)_{8.0}$ intermediate between $La_{8.0}$ and $Ce_{8.0}$, and depletion in $K_{8.0}$ that increases with distance from the plume channel.

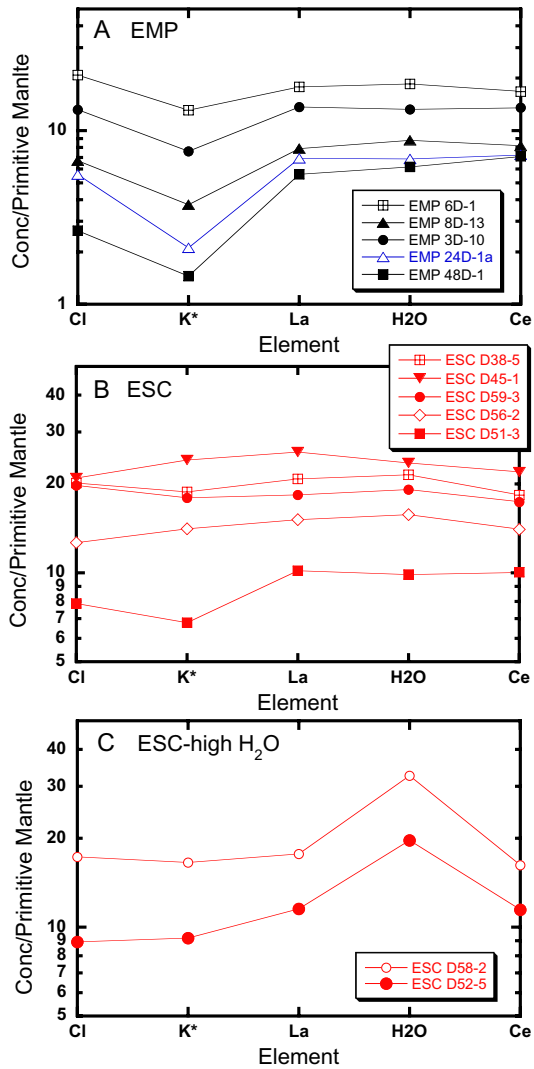

Figure 13. Primitive mantle-normalized trace element concentrations shown in order of relative incompatibility for representative samples from (a) EMP, (b) ESC, and (c) ESC showing glasses with anomalously high H_2O/Ce. Primitive mantle concentrations used for normalization are Cl = 17 ppm, K = 230 ppm, La = 687 ppm, H_2O = 330 ± 50 ppm, and Ce = 1.775 ppm [*Sun and McDonough*, 1989; *McDonough and Sun*, 1995; *Dixon and Clague*, 2001]. Correction procedure of measured trace element concentrations to a parental magma with MgO = 8.0 wt % are described in the caption to Table 1. ESC samples that have previously been identified as having degassed/assimilated water or Cl are excluded from these diagrams.

[33] Normalized ESC parental magma compositions are characterized by relatively flat patterns, with normalized concentrations of $(H_2O)_{8.0}$ intermediate between $La_{8.0}$ and $Ce_{8.0}$ and of $Cl_{8.0}$ at or below $La_{8.0}$ concentrations. The two high $(H_2O)_{8.0}$

Table 1. Calculated Parental Magmatic, Primary Magmatic, and Mantle Trace Element and Volatile Concentrations in End-Member EMP-ESC Compositions[a]

Source $^{206}Pb/^{204}Pb$		DMM 17.5	EPR 18.2	SyG 20.5
Parental magma	MgO	8	8	8
	Ce	3 ± 0.5	7 ± 1	48 ± 4
	H_2O	450 ± 70	1000 ± 150	10,000 ± 1500 (1.0 wt %)
	La	0.8 ± 0.1	2.2 ± 0.4	22.1 ± 3.3
	Cl	15 ± 2	40 ± 10	575 ± 8 5
Primitive magma	MgO	10 ± 2	10 ± 2	12 ± 2
	Ce	2.8 ± 0.13	6.5 ± 1.1	41.0 ± 7.0
	H_2O	420 ± 70	930 ± 160	9300 ± 1600
	La	0.74 ± 0.13	2.0 ± 0.4	18.9 ± 3.2
	Cl	14 ± 2	37 ± 10	490 ± 83
Mantle	%melting	12 ± 2	12 ± 2	8 ± 2
	Ce	0.4 ± 0.1	0.9 ± 0.2	3.8 ± 1.1
	H_2O	54 ± 12	120 ± 27	750 ± 210
	La	0.09 ± 0.02	0.25 ± 0.06	1.64 ± 0.46
	Cl	1.7 ± 0.4	4.5 ± 1.4	40 ± 11

[a] All concentrations in ppm. $^{206}Pb/^{204}Pb$ composition for DMM and SyG end-members is from *Kingsley and Schilling* [1998] and for average EPR is from *Mahoney et al.* [1994]. Correction of measured trace element concentrations to parental magma compositions with MgO = 8.0 wt % for glass compositions with MgO < 8.0 wt % is done using the equation Log $(X)_{8.0}$ = Log (X) − 0.11 * (8-MgO), where X = La, H_2O, Ce, or Cl [*Langmuir et al.*, 1992]. The coefficient of 0.11 is used for the four trace elements because they are all moderately to highly incompatible. For glass compositions with MgO > 8.0 wt %, trace element concentrations are corrected to MgO = 8.0 wt % using the equation $(X)_{8.0} = X/(1.268-0.033 * \text{MgO})$ derived from the change in incompatible element concentrations in Hawaiian lavas during olivine fractionation [*Clague et al.*, 1991 and 1995]. Correction of parental magma to primary magma compositions were done assuming olivine fractionation. Using the results of *Clague et al.* [1991; 1995], trace element concentrations in DMM and EPR parental magmas were multiplied by 0.927 to correct to a primary magma MgO content of 10 wt % and in SyG parental magmas were multiplied by 0.854 to correct a primary magma MgO content of 12 wt %. Mantle compositions calculated using the batch melting equation and bulk partition coefficients (D_0) of 0.013 for Ce, 0.010 for H_2O [*Dixon et al.*, 1988], 0.008 for La, and 0.002 for Cl [*Schilling et al.*, 1980]. Uncertainties are ±15% for the estimate of end-member compositions, ±7% for correction to primary magma compositions, and ±16% or ±23% for extent of partial melting for the DMM/EPR or SyG end-members.

samples have high $(H_2O)_{8.0}$ relative to $La_{8.0}$ and $Ce_{8.0}$ but otherwise flat patterns. Parental magmas closer to the SyG plume (GLO7 D38-5 and D45-1) have some of the highest absolute concentrations of $(H_2O)_{8.0}$ (1 wt % and above) but exhibit no enrichments in water relative to $La_{8.0}$ and $Ce_{8.0}$ (Figure 13b). The coupled behavior of $(H_2O)_{8.0}$ and $Ce_{8.0}$ in the Salas *y* Gomez plume is similar to that observed for MORB [*Dixon et al.*, 1988; *Michael*, 1995; *Danyuschevsky et al.*, 2000; *Simons*, 2000; *Dixon and Clague*, 2001]. This is an important result of this study because we can say with certainty that water is not decoupled from nonvolatile incompatible elements during formation of the SyG plume.

5.1.2. $Ce_{8.0}$, $(H_2O)_{8.0}$ and $Cl_{8.0}$ concentrations in parental magmas

[34] $Ce_{8.0}$, $(H_2O)_{8.0}$, and $Cl_{8.0}$ concentrations in parental magmas are listed in Tables 1 and 2 of auxiliary material and shown as a function of $^{206}Pb/^{204}Pb$ [*Kingsley and Schilling*, 1998], an indicator of the proportion of the SyG plume component, in Figures 14a–14c. Correction methods for shallow fractionation are given in the caption to Table 1. Samples that have degassed or assimilated water and/or chlorine are omitted from the figures.

[35] The radiogenic isotopic characteristics of end-member DMM and SyG mantle sources for the EMP-ESC region have been defined by linear mixing arrays within radiogenic isotope-isotope space. For example, $^{87}Sr/^{86}Sr$ and $^{206}Pb/^{204}Pb$ isotopic compositions of EMP [*Fontignie and Schilling*, 1991; *Hanan and Schilling*, 1989] and ESC [*Kingsley and Schilling*, 1998; *Kingsley*, 2002] glasses form a binary mixing array between DMM and SyG end-members (Figure 15). *Kingsley and Schilling* [1998] define the mantle end-member $^{206}Pb/^{204}Pb$ isotopic compositions to be 17.5 for DMM and 20.5 for SyG. Although the SyG end-member lies just outside the range for C (slightly more radiogenic lead), we believe the plume mantle is dominated by C, rather than recycled material (HIMU and EM1). We also introduce an intermediate component,

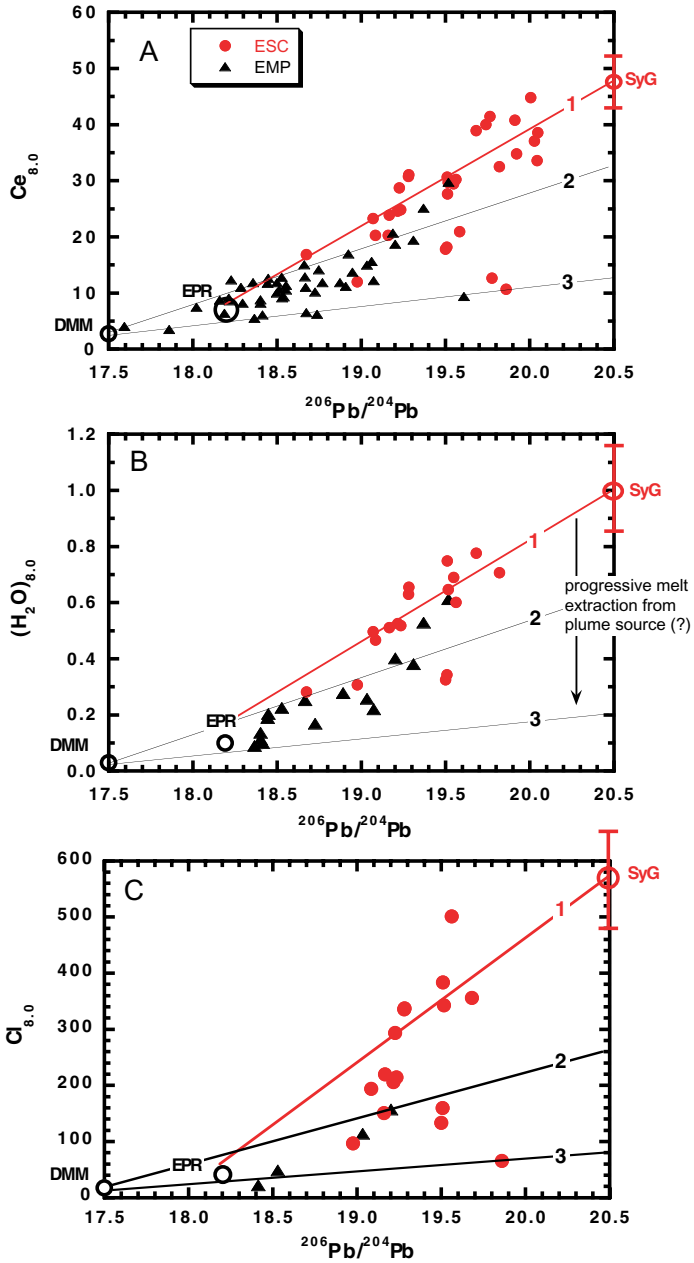

Figure 14. (a) Plot of $Ce_{8.0}$ versus $^{206}Pb/^{204}Pb$. (b) Plot of $(H_2O)_{8.0}$ versus $^{206}Pb/^{204}Pb$. (c) Plot of $Cl_{8.0}$ versus $^{206}Pb/^{204}Pb$. Samples that have been identified as having lost or gained water (in Figure 14b) and Cl (in Figure 14c) have been excluded. $(X)_{8.0}$ was calculated as described in the caption to Table 1. DMM and SyG end-members ($^{206}Pb/^{204}Pb$ = 17.5 and 20.5, respectively) from *Kingsley and Schilling* [1998]. Average EPR ($^{206}Pb/^{204}Pb$ = 18.2) from *Mahoney et al.* [1994]. $(H_2O)_{8.0}$ concentrations in DMM and EPR end-members are calculated based on trends in the $Ce_{8.0}$ data and the assumption that the MORB lavas have H_2O/Ce = 150. Line 1 on Figures 14a, 14b, and 14c are linear fits to ESC data having H_2O > 0.4 wt % and are used to estimate $Ce_{8.0}$, $(H_2O)_{8.0}$, and $Cl_{8.0}$ in the SyG end-member. Line 3 on Figure 14a is a linear fit through the lower limit of the $Ce_{8.0}$ data (samples EN113-4D-1, 5D-1, 26D-1, 28D-1, 30D-1, 34D-1, and 38D-11) and is used to calculate $Ce_{8.0}$, $(H_2O)_{8.0}$, and $Cl_{8.0}$ in the DMM end-member. Line 3 on Figure 14b is calculated from Figure 14a and H_2O/Ce = 150. Line 3 on Figure 14c is calculated from a fit to the lower limit of the $La_{8.0}$ data (not shown) and Cl/La = 17. Line 2 is drawn by eye to illustrate progressive depletion in incompatible elements of the SyG end-member by melting and melt extraction during ascent and migration toward the ridge. Uncertainties in $Ce_{8.0}$, $(H_2O)_{8.0}$, and $Cl_{8.0}$ estimates are shown as error bars for SyG and are within the circular symbol for DMM and EPR. EMP East and West Rift samples are all shown as solid black triangles.

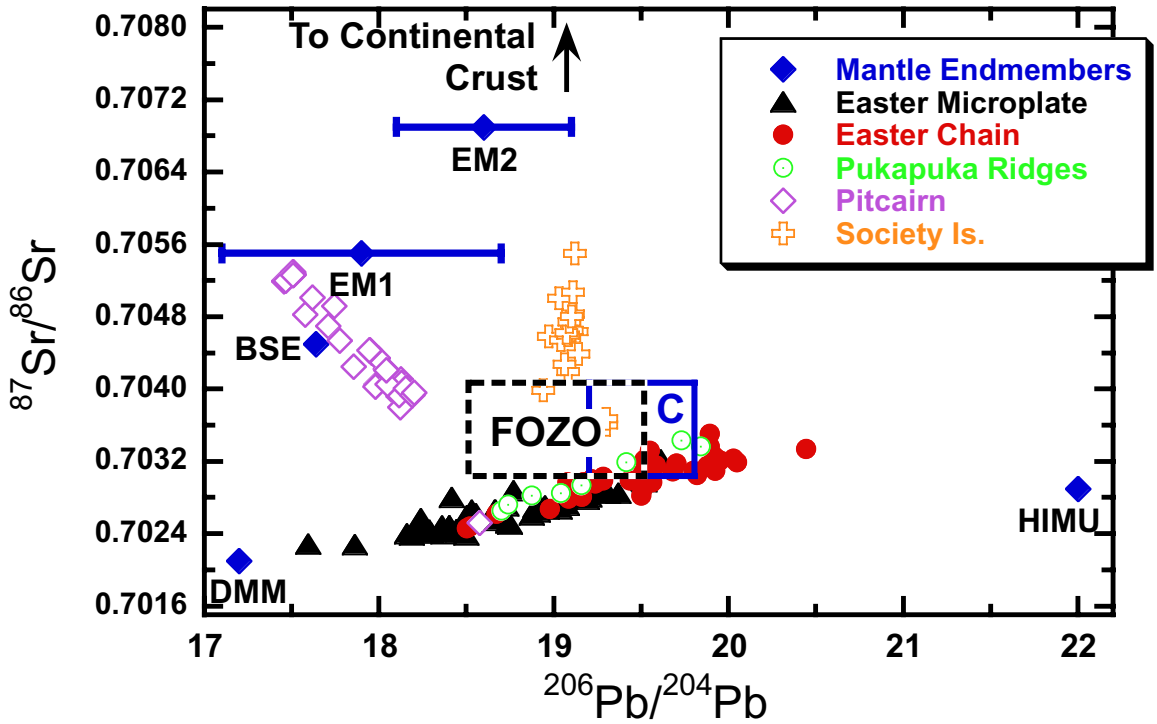

Figure 15. Plot of $^{87}Sr/^{86}Sr$ versus $^{206}Pb/^{204}Pb$ for mantle end-members (HIMU, EM1, EM2, and DMM [*Hofmann*, 1997]) with estimates of FOZO [*Hauri et al.*, 1994] and "C" [*Hanan and Graham*, 1996]. Isotopic data for various ocean island suites are plotted within the end-member framework, with isotopic compositions of the EMP-ESC glasses lying on a binary mixing array between DMM and the ESC plume source (C-HIMU-EM1 mixture). Error bars in $^{206}Pb/^{204}Pb$ for end-members EM1 and EM2 reflect the scatter in Pb data found in ocean islands that represent these end-members. ESC isotopes are from *Kingsley and Schilling* [1998] and *Kingsley* [2002]. EMP isotopes are from *Fontignie and Schilling* [1991] and *Hanan and Schilling* [1989]. Pukapuka data from *Janney et al.* [2000], Pitcairn from *Woodhead and Devey* [1993], Society from *Hemond et al.* [1994].

EPR, representing average depleted East Pacific Rise mantle having $^{206}Pb/^{204}Pb$ = 18.2 [*Mahoney et al.*, 1994]. Data from other Pacific oceanic island or seamount chains are shown for comparison to EMP-ESC [*Janney et al.*, 2000; *Woodhead and Devey*, 1993; *Hemond et al.*, 1994].

[36] In general, parental magmatic $Ce_{8.0}$, $(H_2O)_{8.0}$, and $Cl_{8.0}$ concentrations are high in ESC basalts and low in EMP basalts, consistent with mixing of incompatible-element-depleted DMM and incompatible-element-enriched SyG mantle components [*Pan and Batiza*, 1998] (Figures 14a–14c). In contrast to the single linear mixing arrays on radiogenic isotope-isotope plots (Figure 16), however, $Ce_{8.0}$, $(H_2O)_{8.0}$, and $Cl_{8.0}$ data do not fall on a single linear mixing array. Parental magmas for most ESC samples and the EMP samples nearest the plume channel form a linear array (line 1 on Figures 14a and 14b) with $^{206}Pb/^{204}Pb$ of 19.0–20.0, $Ce_{8.0}$ of 20–45 ppm, $(H_2O)_{8.0}$ of 0.4–0.9, and $Cl_{8.0}$ of 150–400 ppm. Extrapolation of a line fit through the ESC parental magma data with $(H_2O)_{8.0}$ greater than 0.4 wt % yields an estimated SyG parental magma composition of ~48 ± 4 ppm $Ce_{8.0}$, ~1.00 ± 0.15 wt % $(H_2O)_{8.0}$, and ~575 ± 85 ppm $Cl_{8.0}$ (Table 1). Uncertainty in the SyG parental magma composition is estimated to be ±15% based on uncertainty in the slope of the linear regression.

[37] Parental magmas for the EMP and the remaining ESC samples with $(H_2O)_{8.0}$ less than 0.4 wt % (GL07-D32-4, D34-1, D36-1, D51-1, D51-3, D61-2) are bounded by lines having lower slopes (lines 2 and 3) with parental magma compositions ranging between $^{206}Pb/^{204}Pb$ of 17.5–20, $Ce_{8.0}$ of 2–20 ppm, $(H_2O)_{8.0}$ of 0.03–0.4 wt %, and $Cl_{8.0}$ of

<150 ppm. The lower limit (line 3, defined by lower limit of $Ce_{8.0}$ data) could be produced by partial melting of a source composed of a mixture of DMM and a component isotopically similar to the SyG component but with concentrations of incompatible elements lower by a factor of ~4. A parental melt derived from DMM has 3.0 ± 0.5 ppm $Ce_{8.0}$ and 0.045 ± 0.007 wt % $(H_2O)_{8.0}$, and 15 ± 2 ppm $Cl_{8.0}$. A typical EPR parental melt has 7 ± 2 ppm $Ce_{8.0}$ and 0.10 ± 0.02 wt % $(H_2O)_{8.0}$, and 40 ± 10 ppm $Cl_{8.0}$. Thus parental magmas from the SyG component have ~10 times as much $(H_2O)_{8.0}$ as typical EPR parental melts and ~22 times as much as those from the DMM source.

[38] One explanation for the multiple mixing arrays is that the SyG mantle plume source may have undergone variable amounts of melting prior to mixing, thus preserving the radiogenic isotopic composition of the mantle plume component, while reducing the concentration of incompatible elements. This differs slightly from other models involving melting of an upwelling veined mantle plume, as has been proposed to explain similar nonlinear data arrays [*Phipps Morgan*, 1999; *Phipps Morgan and Morgan*, 1999], in which preferential melting of the veins would modify both the incompatible element concentrations and the isotopic composition. The fact that most EMP samples appear to lie on a mixing array with a plume component less enriched in incompatible elements than the initial SyG component is consistent with a model of progressive melt extraction along the flow line from the SyG to the EPR. However, the extent of depletion of the SyG component for ESC samples lying between lines 2 and 3 does not increase systematically with distance from the island of Salas y Gomez; therefore this multistage melting and mixing is not spatially continuous.

5.2. Ce, H_2O, and Cl Concentrations in DMM and SYG Primary Melts

[39] The MgO concentration of primary magma compositions (Table 1), those unmodified by crystallization, are greater than 8.0 wt % and vary as a function of depth and extent of melting [e.g., *McKenzie and Bickle*, 1988; *Niu and Batiza*, 1991; *Langmuir et al.*, 1992]. For the EMP basalts, we assume that primary melts were generated by 10–14% partial melting at pressures of 16 ± 3 kb [*Pan and Batiza*, 1998]. Using the model of *Langmuir et al.* [1992], primary melts generated under these conditions should have ~10 ± 2 wt % MgO, consistent with highest observed MgO-rich compositions. Estimates of depth and extent of melting for plume basalts are more uncertain. Recent work on generation of plume basalts has found that addition of water to an anhydrous mantle source region results in deeper melting and lower mean extents of melting [*Langmuir*, 2000; *Sinton et al.*, 2001]. Generation of the ESC basalts by lower extents of melting than the EMP basalts is also consistent with their alkalic composition [*Green and Ringwood*, 1967] and generation under thicker lithosphere, which tends to prematurely stop melting at the base of the lithosphere [*Langmuir et al.*, 1992]. For these reasons, we assume that primary melts from the SyG plume were generated by 8 ± 2% partial melting at pressures of 20 ± 5 kb [*Pan and Batiza*, 1998]. Primary melts generated under these conditions should have higher MgO contents, ~12 ± 2 wt % [*Langmuir et al.*, 1992]. Differentiation of basaltic melts with MgO > 8.0 wt % usually is dominated by olivine fractionation; therefore the reduction in H_2O and Ce concentrations to correct parental magma compositions back to primitive magma compositions is relatively small (−7% to correct from 8 wt % MgO to 10 wt % MgO; −15% to correct from 8 wt % MgO to 12 wt % MgO [*Clague et al.*, 1995]). Thus primary melts from the SyG source (Table 1) are estimated to have 41 ± 7 ppm Ce, 8500 ± 1500 ppm H_2O, and 490 ± 80 ppm Cl. Primary melts from the average EPR source have 6.5 ± 1.1 ppm Ce, 930 ± 160 ppm H_2O, and 37 ± 10 ppm Cl. Primary melts from the DMM source have 2.8 ± 0.5 ppm Ce, 420 ± 70 ppm H_2O, and 14 ± 2 ppm Cl. Uncertainty in the primitive magma compositions is ±17% (root sum square of ±7% uncertainty in correction to MgO = 8.0 and ±15% uncertainty in the parental magma composition).

5.3. H_2O and Cl Concentrations in DMM, EPR, and SYG Mantle End-Members

[40] Using the batch melting equation, primary magma compositions and extents of melting esti-

mated above, and partition coefficients given in Table 1, we calculate that the SyG source has 3.8 ± 1.1 ppm Ce, 750 ± 210 ppm H_2O, and 40 ± 11 ppm Cl. Average EPR mantle has 0.85 ± 0.20 ppm Ce, 120 ± 27 ppm H_2O, and 4.5 ± 1.4 ppm Cl. The DMM source has 0.37 ± 0.08 ppm Ce, 54 ± 12 ppm H_2O, and 1.7 ± 0.4 ppm Cl. Uncertainty in the mantle composition is estimated to be ±23% for the DMM and EPR sources and ±28% for the SyG source (root sum square of uncertainties in corrections to parental and primary magma compositions and in extent of partial melting).

[41] In general, these estimates agree well with other estimates of mantle volatile concentrations. Our estimated average EPR and DMM mantle Ce concentrations bracket the estimate for depleted MORB mantle (0.54 ppm, GERM database available at http://earthref.org/databases/GERMRD).
Our EPR mantle water concentration is consistent with other estimates based on water concentrations in MORB (100–180 ppm [*Michael*, 1988]), water in mantle minerals from xenoliths (25–175 ppm [*Bell and Rossman*, 1992a, 1992b]), and measurements of electrical conductivity in the Pacific upper mantle [*Lizarralde et al.*, 1995]. Our estimated Cl concentration for EPR mantle is within the range (2–8 ppm) estimated by *Dixon et al.* [1997].

[42] Our estimates of the water concentration in the SyG plume source region are higher than the H_2O concentration for enriched MORB (EMORB) (e.g., 330 ppm for Juan de Fuca [*Dixon et al. 1988*], 250–450 ppm for various places in the Pacific [*Michael*, 1988]) and overlap with estimates for several other plumes, including Hawaii (e.g., 450 ± 190 ppm for Kilauea [*Wallace*, 1998], 525 ± 75 ppm for Hawaiian plume-influenced upper mantle at North Arch [*Dixon et al.*, 1997]) and the Azores hot spot (∼700 ppm; Asimow et al., manuscript in preparation, 2002). Our calculated SyG mantle Cl concentration (40 ± 11 ppm) is similar to estimates for the refertilized upper mantle source of the North Arch volcanic field lavas north of Hawaii (30 ± 6 ppm [*Dixon et al.*, 1997]), and higher than EMORB (23–30 ppm [*Michael and Schilling*, 1989]).

[43] A concentration of ∼750 ± 210 ppm H_2O in the SyG mantle plume is within estimates of what can be accommodated in nominally anhydrous minerals. It does not require the presence of a hydrous phase, as has been proposed for the northeast Pacific [e.g., *Michael and Chase*, 1987; *Michael*, 1988; *Allan et al.*, 1993; *Cousens et al.*, 1995]. Natural samples have been observed to accommodate up to ∼1000 ppm water bound as OH groups [*Aines and Rossman*, 1984; *Skogby et al.*, 1990; *Smyth et al.*, 1991; *Bell and Rossman*, 1992a, 1992b]. The uncertainty involved in estimating how much H_2O can fit into the structure of these phases under increasing pressures or determining H_2O loss due to perturbations during transport of these minerals to the surface [*Mackwell and Kohlstedt*, 1990] means that estimates of H_2O in nominally anhydrous minerals are minimum estimates.

5.4. Origin of Water in Plumes

[44] It has long been recognized that ocean island basalts (OIB) are enriched in volatiles relative to depleted mid-oceanic ridge basalts (MORB), giving rise to speculation that excess magmatism associated with plumes is related to a mantle "wet spot" [*Schilling et al.*, 1980] or a "not-so-hot spot" [*Bonatti*, 1990]. The origin of higher volatile concentrations, however, remains controversial. Explanations for magmatic and mantle volatile concentrations include the following: process 1, addition of volatiles to magmas by seawater assimilation [e.g., *Rison and Craig*, 1983; *Kyser and O'Neil*, 1984; *Kent et al.*, 1999a, 1999b]; process 2, loss of volatiles from magmas due to shallow degassing effects [e.g., *Dixon et al.* 1991; *Clague et al.*, 1995; *Wallace and Anderson*, 1998]; process 3, addition of volatiles to mantle source regions through redox melting at the interface of relatively reduced ambient mantle with more oxidized subducted lithosphere [e.g., *Green and Falloon*, 1998]; process 4, depletion of volatiles from mantle source regions by devolatilzation reactions and/or progressive melting [*Garcia et al.*, 1989; *Ito et al.*, 1999; *Wyllie and Ryabchikov*, 2000]; process 5, incorporation of recycled hydrated or dehydrated lithospheric components from subduction zones within mantle plumes [e.g., *Kingsley and Schilling*, 1995]; and process 6, incorporation of less-depleted, relatively "undegassed" or "juvenile," volatile-rich

mantle into the mantle plume [e.g., *Kurz et al.*, 1982; *Allègre et al.*, 1983, 1987; *Bell*, 1996].

[45] Detailed studies of submarine oceanic island basalts show that samples affected by assimilation and degassing (processes 1 and 2) can be identified and filtered out of the data set used to constrain primary magmatic and mantle volatile concentrations [*Moore*, 1965; *Moore and Schilling*, 1973; *Unni and Schilling*, 1978; *Clague et al.*, 1991; *Dixon et al.*, 1991, 1997; *Kent et al.*, 1999a, 1999b; *Dixon and Clague*, 2001; this study].

[46] Processes 3 (redox melting) and 4 (devolatilization during ascent) should result in decoupling of volatile and lithophile elements, such as H_2O from Ce. If the high volatile concentrations of the SyG plume were the result of reaction with a deep mantle fluid, we would expect to see a positive H_2O anomaly on the primitive-mantle-normalized trace element plots. The fact that H_2O and the LREE remain coupled with the same relative incompatibilities as observed for MORBs argues against a deep fluid source for the volatiles. Similarly the coupled behavior of H_2O and LREE over the long distance of the Easter plume channel suggests that the water-rich plume material is able to rise and mix with the ambient depleted mantle without extraction of water during incipient melting of the plume ("dehydration melting" [*Ito et al.*, 1999]) or formation of carbonate- and water-rich fluids [*Wyllie and Ryabchikov*, 2000]. Thus we can exclude processes 3 and 4.

[47] Distinguishing between processes 5 (recycled water) and 6 ("juvenile" water) is more difficult [e.g., *Kingsley et al.*, 2002]. Assuming that water is dominantly recycled (process 5), there are three possible ways to modify the relative concentrations of water and lithophile incompatible elements: process 5a, subduction is not efficient at removing water from the hydrated slab, enriching water relative to LREEs; process 5b, subduction is efficient at stripping water from the slab, depleting water relative to LREEs; and process 5c, there is an exact balance between water added during maturation of the lithosphere and removed during subduction and dehydration, with no preferential enrichment or depletion of water relative to LREEs (scenario 5.3).

[48] Process 5a leads to a net flux of water into the mantle. It has been proposed that this extra water could be accommodated within "Dense Hydrous Magnesium Silicates" (DHMS) [e.g., *Ringwood and Major*, 1967; *Yamamoto and Akimoto*, 1977; *Ahrens*, 1989; *Kanazaki*, 1991; *Thompson*, 1992; *Gasparik*, 1993; *Luth*, 1995; *Bose and Navrotsky*, 1998], which can accommodate many weight percent H_2O. The amount of H_2O subducted will vary with the *P-T-t* conditions in each subduction zone but is enhanced by fast subduction rates and subduction of old, cold slabs. If a slab is processed through a relatively cool subduction zone (50 Ma or older [*Staudigel and King*, 1992; *Thompson*, 1992; *Peacock*, 1996]), serpentinized peridotites (antigorite assemblages) may be stable well into eclogite facies conditions [*Scambelluri et al.*, 1995], transfering water to depths where DHMS phases are stable. Recycling of hydrated ultramafics would allow large quantities of H_2O to be subducted without high concentrations of other trace elements, enriching water relative to La and Ce, but affecting little else. This would result in trace element patterns possibly interpretable as recycled crust ± sediment with anomalously high water. This sort of relative enrichment in water has been identified in subduction zone magmas [e.g., *Danyuschevsky et al.*, 1993; *Sisson and Layne*, 1993; *Stolper and Newman*, 1994] but has not yet been identified in ocean islands, and does not characterize the main component of the SyG plume. Therefore process 5a seems unlikely.

[49] Process 5b would result in a net flux of water out of the mantle and into the suprasubduction zone mantle wedge, arc volcanics, and eventually the oceans and atmosphere. Recent studies of natural eclogites exposed in metamorphosed alpine complexes [e.g., *Nadeau et al.*, 1993] support the idea that dehydration is fairly efficient during subduction. Using estimates of dehydration efficiency at convergent margins (~98% water loss during subduction [*Staudacher and Allègre*, 1988]) and trace element concentrations for mature ocean lithosphere from the Global Earth Reference Model (GERM), we can estimate the water content of lithosphere that has passed through the subduction-dehydration zone. Ninety-eight percent dehydration of mature

oceanic crust initially containing ~3 wt % H_2O [*Peacock*, 1990] and a Ce concentration of 6 ppm, results in dehydrated oceanic crust having a H_2O/Ce of ~100. This low H_2O/Ce "recycled" component corresponds well to estimates of several recently described, relatively dry, mantle plume components, including Macdonald Seamount (H_2O/Ce ~128 [*Simons et al.*, 1999]), Foundation seamounts (H_2O/Ce ~130 [*Simons et al.*, 1999]), the Koolau component in Hawaii (H_2O/Ce ~110 [*Dixon and Clague*, 2001]), and the Discovery component in the south Atlantic [*Leist et al.*, 2001; *Dixon et al.*, 2002]. These relatively dry components have water concentrations lower than that predicted from their LREE concentrations (decoupling of water from the LREE). In contrast, the SyG plume has H_2O/Ce twice as high as our estimated dehydrated recycled crustal component and does not display anomalous depletion in water relative to the LREEs. Therefore the volatile signature for the ESC is not likely dominated by an extremely dehydrated recycled component (process 5b).

[50] Process 5c would maintain coupling between water and LREE concentrations via an exact balance of hydration addition and subduction removal of water. This seems unlikely, but ruling it out unequivocally would require quantification of the proportions of various components within the SyG plume. The radiogenic isotopic composition of the SyG plume end-member is consistent with involvement of a recycled crustal component [e.g., *Kingsley and Schilling*, 1998; *Cheng et al.*, 1999; *Kingsley*, 2002] (Figure 15); however, the exact proportion of various end-members is still uncertain. Existing work suggests recycled material in plumes makes up a small proportion [*Lassiter and Hauri*, 1998; *Blichert-Toft et al.*, 1999; *Andres*, 2001] and that the majority of plume material is a nonrecycled mantle material (FOZO, C, PHEM, or depleted mantle). If plume water is dominated by recycled water, then all other volatiles should also be consistent with this scenario. The δD composition of the SyG end-member (−40‰ [*Kingsley et al.*, 2002]) can be explained by either recycled or juvenile water. The strongest evidence against derivation of most of the volatiles from recycled oceanic crust are the elevated $^3He/^4He$ ratios in the SyG component, up to 17.5 times the atmospheric value [*Poreda et al.*, 1993a, 1993b; Poreda, unpublished manuscript, 2002]. Thus high $^3He/^4He$ ratios are problematic for process 5c.

[51] For these reasons, we believe the volatile signature in the ESC is dominated by juvenile volatiles (process 6) rather than recycled material (process 5). Our preferred model has the SyG plume composed dominantly of a less depleted, common mantle plume component plus some fraction (<25%) of a recycled component [*Kingsley and Schilling*, 1998; *Cheng et al.*, 1999; *Kingsley*, 2002]. The similarity in mantle water concentrations for several different C-type plumes (Azores; KEA component in Hawaii) having elevated $^3He/^4He$ ratios leads us to conclude that the water in these plumes is largely juvenile mantle water. A primary origin for water in mantle plumes is consistent with recent wet accretion models for the Earth [*Abe et al.*, 2000]. Thus we speculate that the common mantle plume component has roughly 700 ppm H_2O and H_2O/Ce of ~210.

6. Conclusions

[52] Volatiles in basalts from the Easter Microplate and Easter-Salas y Gomez Seamount Chain are controlled primarily by source heterogeneity and magmatic processes (melting and crystallization), with the relative importance of secondary processes (assimilation and degassing) differing for each region. Gradients in H_2O and Cl concentrations for the seamount samples have maximum values near longitude 106°W (near Salas y Gomez) and progressively decrease toward the east rift of the microplate, mimicking trends of radiogenic isotopes and other nonvolatile, incompatible elements. Nearly constant ratios of H_2O/Ce and Cl/La for most samples within the sample suite indicate that (1) both water and Cl concentrations reflect magmatic values with little shallow assimilation and (2) volatile enrichment of the plume source is related to mantle fertility and not recycling of hydrated oceanic crust. Samples with low H_2O/Ce are the result of degassing, which has resulted in loss of H_2O from mostly differentiated and shallowly erupted samples. Two high H_2O/Ce ESC glasses suggest

the existence of a hydrous component, most likely hydrated peridotite within the lithosphere that was assimilated during magma ascent.

[53] Water concentrations in the EMP basalts are dominated by variations in the proportion of the Salas y Gomez plume component. The maximum H_2O concentration in basalts from the east rift of the Easter Microplate is at ~27°S, where the plume channel intersects the ridge, and decreases to normal MORB values to the north and south of that latitude. Degassing affects only CO_2, which has degassed incompletely from all samples resulting in glasses that are supersaturated with respect to a CO_2-rich vapor phase at the depth of collection. Cl data are more scattered and are controlled dominantly by variable amounts of shallow assimilation of a hydrothermal component. A positive correlation between H_2O/Ce and Cl/La indicates that assimilation of up to 400 ppm H_2O occurred in some of the most depleted samples.

[54] Our data are consistent with generation of EMP-ESC magmas by melting of a mantle source formed by binary mixing between an incompatible and volatile element enriched plume source, located near the islet of Salas y Gomez, and a more depleted MORB source. Estimated mantle volatile concentrations are 750 ± 210 ppm H_2O and 40 ± 11 ppm Cl for the SyG source, 120 ± 27 ppm H_2O and 4.5 ± 1.4 ppm Cl for an average EPR source, and 54 ± 12 ppm H_2O and 1.7 ± 0.4 ppm Cl for the DMM source. We see no preferential enrichment or depletion in H_2O relative to other similarly incompatible elements, suggesting sampling of a source region dominated by more fertile mantle, rather than recycled crust.

Acknowledgments

[55] This research was made possible by NSF grant OCE-9530373 to J.E.D. Helpful reviews by L. Danyschevsky, Y. Tatsumi, and editor B. White greatly improved the manuscript.

References

Abe, Y., E. Ohtani, T. Okuchi, K. Righter, and M. Drake, Water in the early Earth, in *Origin of the Earth and Moon*, edited by R. M. Canup, et al., pp. 414–431, Univ. of Arizona Press, Tucson, 2000.

Agrinier, P. H., R. Hékinian, D. Bideau, and M. Javoy, O and H stable isotope compositions of oceanic crust and upper mantle rocks exposed in the Hess Deep near the Galapagos Triple Junction, *Earth Planet. Sci. Lett.*, *136*, 183–196, 1995.

Ahrens, T. J., Planetary origins: Water storage in the mantle, *Nature*, *342*, 122–123, 1989.

Aines, R. D., and G. R. Rossman, The water content of mantle garnets, *Geology*, *12*, 720–723, 1984.

Allan, J. F., R. L. Chase, B. Cousens, P. J. Michael, M. P. Gorton, and S. D. Scott, The Tuzo Wilson Volcanic Field, NE Pacific: Alkaline volcanism at a complex, diffuse, transform-trench-ridge triple junction, *J. Geophys. Res.*, *98*, 22,367–22,387, 1993.

Allègre, C. J., T. Staudacher, P. Sarda, and M. Kurz, Constraints on evolution of Earth's mantle from rare gas systematics, *Nature*, *303*, 762–766, 1983.

Allègre, C. J., T. Staudacher, and P. Sarda, Rare gas systematics: Formation of the atmosphere, evolution and structure of the Earth's mantle, *Earth Planet. Sci. Lett.*, *81*, 127–150, 1987.

Allègre, C. J., J. P. Poirier, E. Humler, and A. W. Hofmann, The chemical composition of the Earth, *Earth Planet. Sci. Lett.*, *134*, 515–526, 1995.

Andres, M., Hafnium isotope ratio in mid-ocean ridge basalts: a global survey and a focus on the Southern Mid-Atlantic Ridge (40°S–55°S), Master's Thesis, Univ. of Rhode Island, Narragansett, R.I., 2001.

Bell, D. R., Is there a global H-cycle? Evidence from H_2O and trace element systematics of Earth reservoirs, *EOS Trans. AGU*, *77*(46), F806, Fall Meeting Suppl., 1996.

Bell, D. R., and G. R. Rossman, Water in the Earth's mantle: the role of nominally anhydrous minerals, *Science*, *255*, 1391–1397, 1992a.

Bell, D. R., and G. Rossman, The distribution of hydroxyl in garnets from the subcontinental mantle of southern Africa, *Contrib. Mineral. Petrol.*, *111*, 161–178, 1992b.

Blichert-Toft, J., F. A. Frey, and F. Albarède, Hf isotope evidence for pelagic sediments in the source of Hawaiian basalts, *Science*, *285*, 879–882, 1999.

Bonatti, E., Not so hot "hotspots" in the oceanic mantle, *Science*, *250*, 107–111, 1990.

Bonatti, E., C. G. A. Harison, D. E. Fisher, J. Honnorez, J.-G. Schilling, J. J. Stipp, and M. Zentilli, Easter volcanic chain (Southeast Pacific): A mantle hot line, *J. Geophys. Res.*, *82*, 2457–2478, 1977.

Bose, K., and A. Navrotsky, Thermochemistry and phase equilibria of hydrous phases in the system MgO-SiO_2-H_2O: Implications for volatile transport to the mantle, *J. Geophys. Res.*, *103*, 9713–9719, 1998.

Cashman, K. V., and M. T. Mangan, Physical aspects of magmatic degassing, II, Constraints on vesiculation processes from textural studies of eruptive products, *MSA Rev. Mineral.*, *30*, 447–478, 1994.

Chauvel, C., A. W. Hofmann, and P. Vidal, HIMU-EM: The French Polynesian connection, *Earth Planet. Sci. Lett.*, *110*, 99–119, 1992.

Cheng, Q. C., J. D. Macdougall, and P. Zhu, Isotopic constraints on the Easter Seamount Chain source, *Contrib. Mineral. Petrol.*, *135*, 225–233, 1999.

Clague, D. A., W. S. Weber, and J. E. Dixon, Picritic glasses from Hawaii, *Nature*, *353*, 553–556, 1991.

Clague, D. A., J. G. Moore, J. E. Dixon, and W. B. Friesen, Petrology of submarine lavas from Kilauea's Puna Ridge, Hawaii, *J. Petrol.*, *36*, 299–349, 1995.

Clark, J. G., and J. Dymond, Geochronology and petrochemistry of Easter and Sala y Gomez Islands: Implications for the origin of the Sala y Gomez Ridge, *J. Volcanol. Geotherm. Res.*, *2*, 29–48, 1977.

Cousens, B. L., J. F. Allan, M. I. Leybourne, R. L. Chase, and N. Van Wagoner, Mixing of magmas from enriched and depleted mantle sources in the northeast Pacific: West Valley segment, Juan de Fuca Ridge, *Contrib. Mineral. Petrol.*, *120*, 337–357, 1995.

Danyushevsky, L. V., T. J. Falloon, A. V. Sobolev, A. J. Crawford, M. Carroll, and R. C. Price, The H_2O content of basalt glasses from Southwest Pacific back-arc basins, *Earth Planet. Sci. Lett.*, *117*, 347–362, 1993.

Danyuschevsky, L. V., S. M. Eggins, T. J. Falloon, and D. M. Christie, H_2O abundance in depleted to moderately enriched mid-ocean ridge magmas, Part I, Incompatible behaviour, implications for mantle storage, and origin of regional variations, *J. Petrol.*, *41*, 1329–1364, 2000.

Des Marais, D. J., and J. G. Moore, Carbon and its isotopes in mid-oceanic basaltic glasses, *Earth Planet. Sci. Lett.*, *69*, 43–57, 1984.

Dingwell, D. B., and B. O. Mysen, Effects of water and fluorine on the viscosity of albite melt at high pressure: a preliminary investigation, *Earth Planet. Sci. Lett.*, *74*, 266–274, 1985.

Dixon, J. E., Degassing of alkalic basalts, *Am. Mineral.*, *82*, 368–378, 1997.

Dixon, J. E., and D. A. Clague, Volatiles in basaltic glasses from Loihi Seamount, Hawaii: Evidence for a relatively dry plume component, *J. Petrol.*, *42*, 627–654, 2001.

Dixon, J. E., and E. M. Stolper, An experimental study of water and carbon dioxide solubilities in Mid-Ocean Ridge Basaltic Liquids, Part II, Applications to degassing, *J. Petrol.*, *36*, 1633–1646, 1995.

Dixon, J. E., E. Stolper, and J. R. Delaney, Infrared spectroscopic measurements of CO_2 and H_2O in Juan de Fuca Ridge basaltic glasses, *Earth Planet. Sci. Lett.*, *90*, 87–104, 1988.

Dixon, J. E., D. A. Clague, and E. M. Stolper, Degassing history of water, sulfur, and carbon in submarine lavas from Kilauea Volcano, Hawaii, *J. Geol.*, *99*, 371–394, 1991.

Dixon, J. E., E. M. Stolper, and J. R. Holloway, An experimental study of water and carbon dioxide solubilities in mid-ocean ridge basaltic liquids, Part I, Calibration and solubility models, *J. Petrol.*, *36*, 1607–1631, 1995.

Dixon, J. E., D. A. Clague, P. Wallace, and R. Poreda, Volatiles in alkalic basalts from the North Arch Volcanic Field, Hawaii: Extensive degassing of deep submarine-erupted alkalic series lavas, *J. Petrol.*, *38*, 911–939, 1997.

Dixon, J. E., L. Leist, C.. Langmuir, and J.-G. Schilling, Efficient dehydration of recycled crust and sediments observed in plume-influenced mid-ocean ridge basalt,, *Nature*, in press, 2002.

Douglass, J., J.-G. Schilling, and D. Fontignie, Plume-ridge interactions of the Discovery and Shona mantle plumes with the southern Mid-Atlantic Ridge (40°–55°S), *J. Geophys. Res.*, *104*, 2941–2962, 1999.

Duncan, R. A., and R. B. Hargraves, Plate tectonic evolution of the Caribbean region in the mantle reference frame, in *The Caribbean-South American Plate Boundary and Regional Tectonics*, edited by W. E. Bonini, R. B. Hargraves, and R. Shagam, pp. 81–93, Geol. Soc. of Am., Boulder, Colo., 1984.

Evans, B. W., D. M. Shaw, and D. R. Haughton, Scapolite stoichiometry, *Contrib. Mineral. Petrol.*, *24*, 293–305, 1969.

Farley, K. A., J. H. Natland, and H. Craig, Binary mixing of enriched and undegassed (primitive?) mantle components (He, Sr, Nd, Pb) in Samoan lavas, *Earth Planet. Sci. Lett.*, *111*, 183–199, 1992.

Fine, G., and E. Stolper, Carbon dioxide in basaltic glasses: Concentrations and speciations, *Earth Planet. Sci. Lett.*, *76*, 263–278, 1986.

Fontignie, D., and J.-G. Schilling, $^{87}Sr/^{86}Sr$ and REE variations along the Easter Microplate boundaries (south Pacific): Application of multivariate statistical analyses to ridge segmentation, *Chem. Geol.*, *89*, 209–241, 1991.

Garcia, M. O., D. W. Muenow, and K. E. Aggrey, Major elements, volatiles, and stable isotope geochemistry of Hawaiian submarine tholeiitic glasses, *J. Geophys Res.*, *94*, 10,525–10,538, 1989.

Gasparik, T., The role of volatiles in the transition zone, *J. Geophys. Res.*, *98*, 4287–4299, 1993.

Gerlach, T. M., Comment on 'Mid-ocean ridge popping rocks: implications for degassing at ridge crests' by P. Sarda and D. Graham, *Earth Planet. Sci. Lett.*, *105*, 566–567, 1991.

Graham, D., and P. Sarda, Reply to comment by T. M. Gerlach on "Mid-ocean ridge popping rocks: implications for degassing at ridge crests," *Earth Planet. Sci. Lett.*, *105*, 568–573, 1991.

Green, D. H., Magmatic activity as the major process in the chemical evolution of the Earth's crust and mantle, *Tectonophysics*, *13*, 47–71, 1972.

Green, D. H., Contrasted melting relations in a pyrolite upper mantle under mid-ocean ridge, stable crust and island arc environments, *Tectonophysics*, *17*, 285–297, 1973.

Green, D. H., and T. J. Falloon, Pyrolite: A Ringwood concept and its current expression, in *The Earth's Mantle: Composition, Structure, and Evolution*, edited by I. Jackson, pp. 311–378, Cambridge Univ. Press, New York, 1998.

Green, D. H., and A. E. Ringwood, The genesis of basaltic magmas, *Contrib. Mineral. Petrol.*, *15*, 103–190, 1967.

Green, D. H., and M. E. Wallace, Mantle metasomatism by ephemeral carbonatite melts, *Nature*, *336*, 459–462, 1988.

Greenland, L. P., A. T. Okamura, and J. B. Stokes, Constraints on the mechanics of the eruption, *U.S. Geol. Soc. Prof. Paper*, *1463*, 155–164, 1988.

Haase, K. M., and C. W. Devey, Geochemistry of lavas from the Ahu and Tupa volcanic fields, Easter Hotspot, southeast Pacific: Implications for intraplate magma genesis near a spreading axis, *Earth Planet. Sci. Lett.*, *137*, 129–143, 1996.

Hanan, B. B., and D. W. Graham, Lead and Helium isotope evidence from oceanic basalts for a common deep source of mantle plumes, *Science*, *272*, 991–995, 1996.

Hanan, B. B., and J.-G. Schilling, Easter microplate evolution: Pb isotope evidence, *J. Geophys. Res.*, *94*, 7432–7448, 1989.

Hart, S. R., Heterogeneous mantle domains: signatures, genesis and mixing chronologies, *Earth Planet. Sci. Lett.*, *90*, 273–296, 1988.

Hart, S. R., E. H. Hauri, L. A. Oschmann, and J. A. Whitehead, Mantle plumes and entrainment: Isotopic evidence, *Science*, *256*, 517–520, 1992.

Hauri, E. H., SIMS investigations of volatiles in volcanic glasses, 2, Isotopes and abundances in Hawaiian melt inclusions, *Chem. Geol.*, *183*, 115–143, 2002.

Hauri, E. H., J. A. Whitehead, and S. R. Hart, Fluid dynamics and geochemical aspects of entrainment in mantle plumes, *J. Geophys. Res.*, *99*, 24,275–24,300, 1994.

Head, J. W., and L. Wilson, Lava fountain heights at Pu'u O'o, Kilauea, Hawaii: indicators of amount and variations of exsolved magma volatiles, *J. Geophys. Res.*, *92*, 13,715–13,719, 1987.

Hemond, C., C. W. Devey, and C. Chauvel, Source compositions and melting processes in the Society and Austral plumes (South Pacific Ocean): Element and isotope (Sr, Nd, Pb, Th) geochemistry, *Chem. Geol.*, *115*, 7–45, 1994.

Herron, E. M., Sea-floor spreading and Cenozoic history of the east-central Pacific, *Geol. Soc. Am. Bull.*, *83*, 1671–1692, 1972.

Hirth, G., and D. L. Kohlstedt, Water in the oceanic upper mantle: implications for rheology, melt extraction and the evolution of the lithosphere, *Earth Planet. Sci. Lett.*, *144*, 93–108, 1996.

Hofmann, A. W., Chemical differentiation of the Earth: The relationship between mantle, continental crust, and oceanic crust, *Earth Planet. Sci. Lett.*, *90*, 297–314, 1988.

Hofmann, A. W., Mantle geochemistry: The message from oceanic volcanism, *Nature*, *385*, 219–229, 1997.

Ito, G., Y. Shen, G. Hirth, and C. J. Wolfe, Mantle flow, melting and dehydration of the Iceland mantle plume, *Earth Planet. Sci. Lett.*, *165*, 81–96, 1999.

Jambon, A., Earth degassing and large-scale geochemical cycling of volatile elements, *Rev. Mineral.*, *30*, 479–517, 1994.

Jambon, A., and J. L. Zimmerman, Water in oceanic basalts: evidence for dehydration of recycled crust, *Earth Planet. Sci. Lett.*, *101*, 323–331, 1990.

Jambon, A., B. Déruelle, G. Dreibus, and F. Pineau, Chlorine and bromine abundance in MORB: The contrasting behaviour of the Mid-Atlantic Ridge and East Pacific Rise and implications for chlorine geodynamic cycle, *Chem. Geol.*, *126*, 101–117, 1995.

Janney, P. E., J. D. Macdougall, J. H. Natland, and M. A. Lynch, Geochemical evidence from the Pukapuka volcanic ridge system for a shallow enriched mantle domain beneath the South Pacific Superswell, *Earth and Planet. Sci. Lett.*, *181*, 47–60, 2000.

Javoy, M., The birth of the Earth's atmosphere: The behaviour and fate of its major elements, *Chem. Geol.*, *147*, 11–25, 1998.

Kamenetsky, V. S., R. Maas, N. Sushchevskaya, M. Norman, I. Cartwright, and A. A. Peyve, Remnants of Gondwanan continental lithosphere in oceanic upper mantle: Evidence from the South Atlantic Ridge, *Geology*, *29*, 243–246, 2001.

Kanazaki, M., Stability of hydrous magnesium silicates in the mantle transition zone, *Phys. Earth Planet. Int.*, *66*, 307–312, 1991.

Kent, A. J. R., D. A. Clague, M. Honda, E. M. Stolper, I. D. Hutcheon, and M. D. Norman, Widespread assimilation of a sea-water-derived component at Loihi Seamount, Hawaii, *Geochim. Cosmochim. Acta*, *63*, 2749–2761, 1999a.

Kent, A. J. R., M. D. Norman, I. D. Hutcheon, and E. M. Stolper, Assimilation of seawater-derived components in an oceanic volcano: Evidence from matrix glasses and glass inclusions from Loihi seamount, Hawaii, *Chem. Geol.*, *156*, 299–319, 1999b.

Kingsley, R. H., Carbon dioxide and water in Mid-Atlantic Ridge basalt glasses, Thesis MS., Univ. of R. I., Narragansett, 1989.

Kingsley, R. H., Mantle plume-spreading ridge interaction in the southeast Pacific: Isotope and trace element geochemistry of the Easter-Salas y Gomez Seamount chain and the Easter Microplate,, Ph.D. Dissertation, Univ. of Rhode Island, Narragansett, 2002.

Kingsley, R. H., and J.-G. Schilling, Carbon in Mid-Atlantic Ridge basalt glasses from 28°N to 63°N: Evidence for a carbon-enriched Azores mantle plume, *Earth Planet. Sci. Lett.*, *129*, 31–53, 1995.

Kingsley, R. H., and J.-G. Schilling, Plume-ridge interaction in the Easter-Salas y Gomez seamount chain-Easter Microplate system: Pb isotope evidence, *J. Geophys. Res.*, *103*, 24,159–24,177, 1998.

Kingsley, R. H., J.-G. Schilling, J. E. Dixon, P. Swart, R. Poreda, and K. Simons, D/H ratios in basalt glasses from the Salas y Gomez mantle plume interacting with the East Pacific Rise: Water from old D-rich recycled crust or primordial water from the lower mantle?, *Geochem. Geophys. Geosyst.*, *3*(4), 10.1029/2001GC000199, 2002. (Available at http://www.g-cubed.org)

Kurz, M. D., W. J. Jenkins, and S. R. Hart, Helium isotopic systematics of oceanic islands and mantle heterogeneity, *Nature*, *297*, 43–47, 1982.

Kushiro, I., Stability of amphibole and phlogopite in the upper mantle, *Carnegie Inst. Washington Yearbook*, *68*, 245–247, 1970.

Kushiro, I., Y. Syono, and S. Akimoto, Melting of a peridotite nodule at high pressures and high water pressures, *J. Geophys. Res.*, *73*, 6023–6029, 1968.

Kyser, T. K., and J. R. O'Neil, Hydrogen isotope systematics of submarine basalts, *Geochim. Cosmochim. Acta*, *48*, 2123–2133, 1984.

Lange, R. A., The effect of H_2O, CO_2 and F on the density and viscosity of silicate melts, in *Volatiles in Magmas, Rev. Mineral.*, edited by M. R. Carroll and J. R. Holloway, vol. 30, pp. 331–369, Mineral Soc. of Am., Washington, D.C., 1994.

Langmuir, C. H., Mantle temperature, water content and mantle flow controls on ridge melting in the vicinity of hot spots,

Physical and Chemical Effects of Mantle Plume, paper presented at Spreading Ridge Interaction Workshop, RIDGE workshop, Troutdale, Oreg., 2000.

Langmuir, C. H., E. M. Klein, and T. Plank, Petrological systematics of mid-ocean ridge basalts: Constraints on melt generation beneath ocean ridges, in *Mantle Flow and Melt Generation at Mid-Ocean Ridges*, *Geophys. Monogr. Ser.*, vol. 71, edited by Jason Phipps Morgan et al., pp. 183–280, AGU, Washington, D.C., 1992.

Lassiter, J. C., and E. H. Hauri, Osmium-isotope variations in Hawaiian lavas: Evidence for recycled oceanic lithosphere in the Hawaiian plume, *Earth Planet. Sci. Lett.*, *164*, 483–496, 1998.

Leist, L., J. Dixon, and J.-G. Schilling, Water concentrations in enriched mantle components in the South Atlantic: Evidence for efficient dehydration or recycled crust and sediments, *Eos Trans. AGU*, *82*(48), Fall Meet. Suppl., F1285, 2001.

Liu, Z. J., The origin and evolution of the Easter Seamount Chain, Doctoral Thesis, Univ. of South Fla., Tampa, 1996.

Lizarralde, D., A. Chave, G. Hirth, and A. Schultz, Northeastern Pacific mantle conductivity profile from long-period magnetotelluric soundings using Hawaii-to-California submarine cable data, *J. Geophys. Res.*, *100*, 17,837–17,854, 1995.

Luth, R. W., Is phase A relevant to the Earth's mantle?, *Geochim. Cosmochim. Acta*, *59*, 679–686, 1995.

Mackwell, S. J., and D. L. Kohlstedt, Diffusion of hydrogen in olivine; implications for water in the mantle, *J. Geophys. Res.*, *95*, 5079–5088, 1990.

Mahoney, J. J., J. M. Sinton, M. D. Kurz, J. D. Macdougall, K. J. Spencer, and G. W. Lugmair, Isotope and trace element characteristics of a super-fast spreading ridge: East Pacific Rise, 13–23 degrees S, *Earth Planet. Sci. Lett.*, *121*, 173–193, 1994.

Mammerickx, J., Depth anomalies in the Pacific: Active, fossil and precursor, *Earth Planet. Sci. Lett.*, *53*, 147–157, 1981.

Mammerickx, J., and D. T. Sandwell, Rifting of old oceanic lithosphere, *J. Geophys. Res.*, *91*, 1975–1988, 1986.

McDonough, W. F., and S.-S. Sun, The composition of the Earth, *Chem. Geol.*, *120*, 223–253, 1995.

McKenzie, D., and M. J. Bickle, The volume and composition of melt generated by extension of the lithosphere, *J. Petrol.*, *29*, 625–679, 1988.

Michael, P., The concentration, behavior and storage of H_2O in the suboceanic upper mantle: Implications for mantle metasomatism, *Geochim. Cosmochim. Acta*, *52*, 555–566, 1988.

Michael, P., Regionally distinctive sources of depleted MORB: Evidence from trace elements and H_2O, *Earth Planet. Sci. Lett.*, *131*, 301–320, 1995.

Michael, P. J., Implications for magmatic processes at Ontong Java Plateau from volatile and major element contents of Cretaceous basalt glasses, *Geochem. Geophys. Geosyst.*, *1* Paper number 1999GC000025, December 13 1999. (Available at http://www.g-cubed.org)

Michael, P., and R. L. Chase, The influence of primary magma composition, H_2O, and pressure on midj-ocean ridge basalt differentiation, *Contrib. Mineral. Petrol.*, *96*, 245–263, 1987.

Michael, P., and W. Cornell, Influence of spreading rate and magma supply on crystallization and assimilation beneath mid-ocean ridges: Evidence from chlorine and major element chemistry of mid-ocean ridge basalts, *J. Geophys. Res.*, *103*, 18,325–18,356, 1998.

Michael, P. J., and J.-G. Schilling, Chlorine in mid-ocean ridge magmas: Evidence for assimilation of seawater-influenced components, *Geochim. Cosmochim. Acta*, *53*, 3131–3143, 1989.

Moore, J. G., Petrology of deep-sea basalt near Hawaii, *Am. J. Sci.*, *263*, 40–52, 1965.

Moore, J. G., and J.-G. Schilling, Vesicles, water, and sulfur in Reykjanes Ridge basalts, *Contr. Mineral. Petrol.*, *41*, 105–118, 1973.

Moore, J. G., J. N. Batchelder, and C. G. Cunningham, CO_2-filled vesicles in mid-ocean basalt, *J. Volcanol. Geotherm. Res.*, *2*, 309–327, 1977.

Morgan, W. J., Deep mantle convection plumes and plate motions, *Am. Assoc. Pet. Geol. Bull.*, *56*, 203–213, 1972.

Naar, D. F., and R. N. Hey, Tectonic evolution of the Easter Microplate, *J. Geophys. Res.*, *96*, 7961–7993, 1991.

Naar, D. F., and P. Wessel, Hotspotting the Easter-Salas y Gomez-Nazca Seamount Chain, *Eos Trans. AGU*, *81*(48), Fall Meet. Suppl., F1374, 2000.

Nadeau, S., P. Philippot, and F. Pineau, Fluid inclusion and mineral isotopic compositions (H-C-O) in eclogitic rocks as tracers of local fluid migration during high-pressure metamorphism, *Earth Planet. Sci. Lett.*, *114*, 431–488, 1993.

Nielsen, R. L., R. E. Sours-Page, and K. S. Harpp, Role of a Cl-bearing flux in the origin of depleted ocean floor magmas, *Geochem. Geophys. Geosyst.*, *1*, Paper number 1999GC000017, May 24, 2000. (Available at http://www.g-cubed.org)

Niu, Y., and R. Batiza, An empirical method for calculating melt compositions produced beneath mid-ocean ridges: Application for axis and off-axis (seamounts) melting, *J. Geophys. Res.*, *96*, 21,753–21,777, 1991.

O'Connor, J. M., P. Stoffers, and M. O. McWilliams, Time-space mapping of Easter Chain volcanism, *Earth Planet. Sci. Lett.*, *136*, 197–212, 1995.

Pan, Y., and R. Batiza, Major element chemistry of volcanic glasses from the Easter Seamount Chain: Constraints on melting conditions in the plume channel, *J. Geophys. Res.*, *103*, 5287–5304, 1998.

Peacock, S. M., Fluid processes in subduction zones, *Science*, *248*, 329–336, 1990.

Peacock, S. M., Thermal and petrologic structure of subduction zones, in *Subduction Top to Bottom*, *Geophys. Monogr. Ser.*, vol. 96, edited by G. E. Bebout et al., pp. 119–133, AGU, Washington, D.C., 1996.

Phipps Morgan, J., Isotope topology of individual hotspot basalt arrays: Mixing curves or melt extraction trajectories?, *Geochem. Geophys. Geosyst.*, *1*, Paper number 1999GC000004, December 13, 1999. (Available at http://www.g-cubed.org)

Phipps Morgan, J., and W. J. Morgan, Two-stage melting and the geochemical evolution of themantle: A recipe for mantle plum-pudding, *Earth Planet. Sci. Lett.*, *170*, 215–239, 1999.

Pichavant, M., H. J. Valencia, S. Boulmier, L. Brique, J.-L. Joron, M. Juteau, L. Marin, A. Michard, S. M. F. Sheppard, M. Treuil, and M. Vernet, The Macusani glasses, SE Peru: Evidence of chemical fractionation in peraluminous magmas, in *Magmatic Processes: Physiochemical Principles*, *Spec. Publ. Geochem. Soc.*, *1*, 359–373, 1987.

Pilger, R. H. J., and D. W. Handschumacher, The fixed-hotspot hypothesis and origin of the Easter-Sala y Gomez-Nazca trace, *Geol. Soc. Amer. Bull.*, *92*, 437–446, 1981.

Pineau, F., and M. Javoy, Carbon isotopes and concentrations in mid-ocean ridge basalts, *Earth Planet. Sci. Lett.*, *62*, 239–257, 1983.

Poreda, R. J., J.-G. Schilling, and H. Craig, Helium and hydrogen isotopes in ocean-ridge basalts north and south of Iceland, *Earth Planet. Sci. Lett.*, *78*, 1–17, 1986.

Poreda, R. J., J.-G. Schilling, R. Batiza, and D. Naar, Geochemistry of volcanism along the Easter Seamount chain, *EOS Trans. AGU*, *74*(43), F672, Fall Meeting Suppl., 1993a.

Poreda, R. J., J.-G. Schilling, and H. Craig, Helium ratios in Easter microplate basalts, *Earth Planet. Sci. Lett.*, *119*, 319–329, 1993b.

Reynolds, J. R., Segment-scale systematics of Mid-Ocean Ridge magmatism and geochemistry, Ph.D. thesis, Columbia Univ., Palisades, New York, 1995.

Richet, P., A.-M. Lejeune, F. Holtz, and J. Roux, Water and the viscosity of andesite melts, *Chem. Geol.*, *128*, 185–197, 1996.

Ringwood, A. E., and A. Major, High-pressure reconnaissance investigations in the system Mg_2SiO_4-MgO-H_2O, *Earth Planet. Sci. Lett.*, *2*, 130–133, 1967.

Rison, W., and H. Craig, Helium isotopes and mantle volatiles in Loihi Seamount and Hawaiian Island basalts and xenoliths, *Earth Planet. Sci. Lett.*, *66*, 407–426, 1983.

Sandwell, D. T., E. L. Winterer, J. Mammerickx, R. A. Duncan, M. A. Lynch, D. A. Levitt, and C. L. Johnson, Evidence for diffuse extension of the Pacific plate from Pukapuka ridges and cross-grain gravity lineations, *J. Geophys. Res.*, *100*, 15,087–15,099, 1995.

Scambelluri, M., O. Muntener, J. Hermann, G. B. Piccardo, and V. Trommsdorff, Subduction of water into the mantle: History of an Alpine peridotite, *Geology*, *23*, 459–462, 1995.

Schilling, J.-G., M. B. Bergeron, and R. Evans, Halogens in the mantle beneath the North Atlantic, *Philos. Trans. R. Soc. London Ser. A*, *297*, 147–178, 1980.

Schilling, J.-G., M. Zalac, R. Evans, T. Johnston, W. White, J. D. Devine, and R. Kingsley, Petrologic and geochemical variations along the Mid-Atlantic Ridge from 29 degrees N to 73 degrees N, *Am. J. Sci.*, *238*, 510–586, 1983.

Schilling, J.-G., H. Sigurdsson, A. N. Davis, and R. N. Hey, Easter microplate evolution, *Nature*, *317*, 325–331, 1985.

Searle, R. C., R. I. Rusby, J. Engeln, J. Zukin, P. M. Hunter, T. P. Le Bas, H.-J. Hoffman, and R. Livermore, Comprehensive sonar imaging of the Easter microplate, *Nature*, *341*, 701–705, 1989.

Searle, R. C., R. T. Bird, R. I. Rusby, and D. F. Naar, The development of two oceanic microplates: Eater and Juan Fernandez microplates, East Pacific Rise, *J. Geol. Soc. London*, *150*, 965–976, 1993.

Sheppard, S. M. F., and S. Epstein, D/H and $^{18}O/^{16}O$ ratios of minerals of possible mantle or lower crustal origin, *Earth Planet. Sci. Lett.*, *9*, 232–239, 1970.

Simons, K. K., Volatiles in basaltic glasses from the Easter-Salas y Gomez seamount chain and Easter microplate: Implications for geochemical cycling of volatile elements, thesis, M.S., University of Miami, Coral Gables, 2000.

Simons, K. K., J. E. Dixon, and C. W. Devey, Volatile contents of basaltic glasses from the Foundation Seamount Chain, *Eos Trans. AGU*, *80*(46), 1091, 1999.

Sinton, J. M., and R. S. Detrick, Mid-ocean ridge magma chambers, *J. Geophys Res.*, *97*, 197–216, 1992.

Sinton, J., R. S. Detrick, J. P. Canales, G. Ito, M. Behn, T. Blacic, B. Cushman, and J. Dixon, Correlated geophysical, geochemical, and volcanological manifestations of plume-ridge interaction along the Galápagos Spreading Center, 90.5–98° W, *Eos Trans. AGU*, *82*(47), F1204, Fall Meeting Suppl., 2001.

Sisson, T. W., and G. D. Layne, H_2O in basalt and basaltic andesite glass inclusions from four subduction-related volcanoes, *Earth Planet. Sci. Lett.*, *117*, 619–635, 1993.

Skogby, H., D. R. Bell, and G. R. Rossman, Hydroxide in pyroxene: Variations in the natural environment, *Am. Mineral.*, *75*, 764–774, 1990.

Smith, W. H. F., and D. T. Sandwell, Bathymetric prediction from dense satellite altimetry and sparse shipboard bathymetry, *J. Geophys. Res.*, *99*, 21,803–21,824, 1994.

Smyth, J. R., D. R. Bell, and G. R. Rossman, Incorporation of hydroxyl in upper-mantle clinopyroxenes, *Nature*, *351*, 732–735, 1991.

Sobolev, A. V., and M. Chaussidon, H_2O concentrations in primary melts from supra-subduction zones and mid-ocean ridges: Implications for H_2O storage and recycling in the mantle, *Earth Planet. Sci. Lett.*, *137*, 45–55, 1996.

Sparks, R. S. J., J. Barclay, C. Jaupart, H. M. Mader, and J. C. Philips, Physical aspects of magmatic degassing I. Experimental and theoretical constraints on vesiculation, *Rev. Mineral.*, *30*, 413–445, 1994.

Stakes, D. S., and J. R. O'Neil, Mineralogy and stable isotope geochemistry of hydrothermally altered oceanic rocks, *Earth Planet. Sci. Lett.*, *57*, 285–304, 1982.

Staudacher, T., and C. J. Allègre, Recycling of oceanic crust and sediments: The noble gas subduction barrier, *Earth Planet. Sci. Lett.*, *89*, 173–183, 1988.

Staudigel, H., and S. D. King, Ultrafast subduction: The key to slab recycling efficiency and mantle differentiation, *Earth Planet. Sci. Lett.*, *109*, 517–530, 1992.

Stolper, E. M., and J. R. Holloway, Experimental determination of the solubility of carbon dioxide in molten basalt at low pressure, *Earth Planet. Sci. Lett.*, *87*, 397–408, 1988.

Stolper, E. M., and S. Newman, The role of water in the Petrogenesis of Mariana Trough magmas, *Earth Planet. Sci. Lett.*, *121*, 293–325, 1994.

Sun, S.-S., Chemical composition and origin of the Earth's primitive mantle, *Geochim. Cosmochim. Acta*, *46*, 179–192, 1982.

Sun, S.-S., and W. F. McDonough, Chemical and isotopic

systematics of oceanic basalts: implications for mantle composition and processes, in *Magmatism in the Ocean Basins*, edited by A. D. Saunders and M. J. Norry, pp. 313–345, *Spec. Pub. Geol. Soc.*, 42, 1989.

Tajika, E., Mantle degassing of major and minor volatile elements during the Earth's history, *Geophys. Res. Lett.*, *25*, 3991–3994, 1998.

Thompson, A. B., Water in the Earth's upper mantle, *Nature*, *358*, 295–302, 1992.

Unni, C. K., and J.-G. Schilling, Cl and Br degassing by volcnism along the Reykjanes Ridge and Iceland, *Nature*, *272*, 19–23, 1978.

Vergniolle, S., and C. Jaupart, Separated two-phase flow and basaltic eruptions, *J. Geophys. Res.*, *91*, 12,842–12,860, 1986.

Vergniolle, S., and C. Jaupart, Dynamics of degassing at Kilauea volcano, Hawaii, *J. Geophys. Res.*, *95*, 2793–2809, 1990.

Wallace, P. J., Water and partial melting in mantle plumes: Inferences from the dissolved H_2O concentrations of Hawaiian basaltic magmas, *Geophys. Res. Lett.*, *25*, 3639–3642, 1998.

Wallace, P. J., and A. T. Anderson Jr., Effects of eruption and lava drainback on the H_2O contents of basaltic magmas at Kilauea Volcano, *Bull. Volcanol.*, *59*, 327–344, 1998.

Weaver, B. L., The origin of ocean island basalt end-member compositions: Trace element and isotopic constraints, *Earth Planet. Sci. Lett.*, *104*, 381–397, 1991.

Webster, J. D., R. J. Kinzler, and E. A. Mathez, Chloride and water solubility in basalt and andesite melts and implications for magmatic degassing, *Geochim. Cosmochim. Acta*, *63*, 729–738, 1999.

Wenner, D. B., and H. P. Taylor, Oxygen and hydrogen isotope studies of the serpentinization of ultramafic rocks in oceanic environments and continental ophiolite complexes, *Am. J. Sci.*, *273*, 207–239, 1973.

White, W. M., and A. W. Hofmann, Sr and Nd isotope geochemistry of oceanic basalts and mantle evolution, *Nature*, *296*, 821–825, 1982.

Wood, B. J., L. T. Bryndzia, and K. E. Johnson, Mantle oxidation state and its relationship to tectonic environment and fluid speciation, *Science*, *248*, 337–345, 1990.

Woodhead, J. D., and C. W. Devey, Geochemistry of the Pitcairn seamounts, I, source character and temporal trends, *Earth Planet. Sci. Lett.*, *116*, 81–99, 1993.

Woods, M. T., and E. A. Okal, The structure of the Nazca Ridge and Sala y Gomez seamount chain from the dispersion of Rayleigh waves, *Geophys. J. Int.*, *117*, 205–222, 1994.

Wyllie, P. J., and I. D. Ryabchikov, Volatile components, magmas, and critical fluids in upwelling mantle, *J. Petrol.*, *41*, 1195–1206, 2000.

Yamamoto, K., and S. Akimoto, The system MgO-SiO_2-H_2O at high pressures and temperatures; stability field for hydroxyl-chondrodite, hydroxyl-clinohumite and 10Å-phase, *Am. J. Sci.*, *277*, 288–312, 1977.

Zindler, A., and S. Hart, Chemical geodynamics, *Ann. Rev. Earth Planet. Sci.*, *14*, 493–571, 1986.

Zindler, A., E. Jagoutz, and S. Goldstein, Nd, Sr and Pb isotopic systematics in a three-component mantle: a new perspective, *Nature*, *298*, 519–523, 1982.